Environmental Drivers of Cyanobacterial Harmful Algal Blooms and Cyanotoxins in Clear Lake: 2020-2021

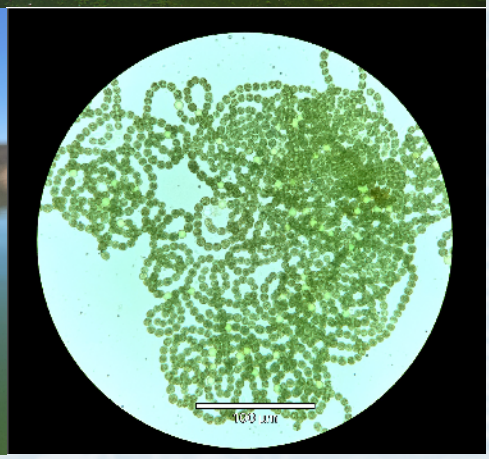

Kyra Florea
Brittany Stewart
Eric Webb
David Caron
Jayme Smith

Southern California Coastal Water Research Project

Technical Report 1261

Environmental Drivers of Cyanobacterial Harmful Algal Blooms and Cyanotoxins in Clear Lake: 2020-2021

Kyra Florea[1], Brittany Stewart[1], Eric Webb[1], David Caron[1], and Jayme Smith[2]

[1] *University of Southern California, Los Angeles, CA*
[2] *Southern California Coastal Water Research Project, Costa Mesa, CA*

June 2022
Technical Report 1261

ACKNOWLEDGEMENTS

This report was produced with funding from, and is a grant deliverable to, the Central Valley Regional Water Quality Control Board, in fulfillment of the agreement "Environmental Drivers of Cyanobacterial Blooms in Clear Lake" (Agreement No. 19-003-150).

The authors thank the Big Valley Band of Pomo Indians and their Environmental Protection Office for sampling assistance. The authors also thank the following individuals for assistance: Christopher Denniston and Gaurav Sukhatme (assistance and data processing for drone sampling and robotics), Amanda Tinoco, Anjali Bhatnagar, Ania Webb, and Gerid Ollison (assistance with field sampling).

Prepared for:

As a deliverable for the Central Valley Regional Water Quality Control Board

"Environmental Drivers of Cyanobacterial Blooms in Clear Lake"

Agreement No. 19-003-150

EXECUTIVE SUMMARY

The chemical, physical, and biological factors (i.e., environmental drivers) leading to cyanobacterial blooms and cyanotoxin production in Clear Lake, CA were examined over a period of two growing seasons in the lake. A combination of observational platforms included a sensor-equipped WireWalker for obtaining continuous vertical profiles of several pertinent environmental parameters, a sensor-equipped autonomous underwater vehicle (YSI i3XO EcoMapper) for obtaining whole-lake vertical profiles of environmental parameters, and a small Unmanned Aerial System (sUAS; a hyperspectral drone) for capturing imagery of surface manifestations and aggregations of cyanobacteria. Combined use of these instruments, coupled to discrete water sampling, provided unprecedented insight for the interpretation of cyanobacterial distributions and cyanotoxin production.

1. A high degree of spatial and temporal variability in cyanoHABs was observed in the study. This was true on an interannual basis, across the three arms of the lake, and on spatial scales as small as meters. The EcoMapper was instrumental in documenting differences between arms of the lake, providing a whole-lake synoptic picture of important chemical, physical, and biological parameters along the main axes of the arms. Data yielded by the robotic instrumentation identified rapid changes (hours to days) in physical forcing and water column mixing in the lake due to wind/wave activity. Periods of intermittent winds and calm periods resulted in rapid response of the biological community affecting concentrations of dissolved oxygen in the lake, particularly near the sediments. The data indicate that a major factor in the stimulation and persistence of cyanobacterial blooms in Clear Lake relates to periods of anoxia (during periods of calm) that reduce dissolved oxygen and may act to release phosphorus from the sediments, followed by periods of active water column mixing (windy periods) which distribute those nutrients throughout the water column.

2. Drone imagery, complemented with discrete sampling at the surface of the lake, captured the nature and magnitude of patchiness exhibited by cyanobacterial blooms. Such patchiness is a major consideration in determining where and how to collect samples for HAB analyses. The precise approach to sampling should be tailored to the specific goal of the monitoring program. For example, the comparison of information obtained by the EcoMapper in Konocti Bay flying at 1.5 m depth, drone imagery, and discrete water samples collected at 1.5 m depth indicate that “average” lake conditions are better served by sampling at a subsurface depth (the EcoMapper indicated less heterogeneity than observed by the drone or onboard personnel. Conversely, surface samples collected within “scums” or “clumps” better represent the extreme toxin concentrations that can exist in these accumulations). Sampling strategy should be guided by programmatic goals and concerns.

3. Significant concentrations of toxin were observed in the middle of the lake throughout the study, although most appear to be modest relative to values that have been obtained from shoreline samples. This is not surprising given the accumulations of material that often occur along shorelines, but quantitative information on mid-lake values have been considerably bolstered by this study.

4. Clear Lake often exhibited chlorophyll *a* concentrations above the TMDL target across weekly and monthly scales. Furthermore, increased microcystin concentrations had a weak, but positive relationship with chlorophyll *a*, suggesting that increased algal biomass generally was related to an increased risk of cyanotoxin presence. In the 2020 August survey, a total of 18% of samples collected were greater than the TMDL target concentration and a majority of those observations were collected in the Lower and Oaks Arms. Exceedances of the TMDL chlorophyll *a* target were observed across multiple months in 2021. Concentrations of chlorophyll *a* exceeded the TMDL target in 76% of samples collected, with at least one station exceeding the target each survey month.

5. Microcystin concentrations have a weak, but positive relationship with higher total nitrogen concentrations and reduced nitrogen-limitation. Qualitatively, nitrogen fixers are more prominent in the early season fitting with priming Clear Lake with nitrogen which subsequently sets the stage for the dominance of *Microcystis*.

6. Molecular analysis of samples revealed cyanobacteria to be the dominant microbial taxa during 2020 and 2021; however, there were noticeable differences between the two years in the composition of the heterotrophic bacteria community. Results from metagenomic assemblies from 2020 and 2021 suggest that *Microcystis* is one of the primary producers of microcystins in Clear Lake.

TABLE OF CONTENTS

LIST OF FIGURES

LIST OF TABLES

INTRODUCTION

Harmful cyanobacterial blooms (cyanoHABs) have gained international attention over the past decade due to increased frequency and severity of these events (Paerl & Paul 2012; Otten & Paerl 2015), particularly in lakes and reservoirs, which contain a large fraction of the world's drinking and irrigation water supply. CyanoHABs cause a large number of water quality issues such as impairment of recreational uses, reduced aesthetics, low dissolved oxygen concentrations, and taste and odor problems in drinking water. However, the production of cyanotoxins is the most concerning issue due to the health impacts these substances pose to humans, domestic pets, wildlife, and livestock (Stewart et al. 2008; Li et al. 2011; Trevino-Garrison et al. 2015).

Clear Lake is the largest natural freshwater lake in California and one of the oldest lakes in North America. The lake is productive and seasonally warm (summer surface water temperatures approaching 30˚C; Mioni & Kudela 2011), but it experiences considerable seasonality and strong wind-induced mixing throughout the year which results in a polymictic lake (Richerson et al. 1994). The lake has also been designated an EPA superfund site due to high levels of mercury associated with the Sulphur Bank Mercury Mine (inactive since 1957) located at the southeastern edge of the Oaks Arm of the lake. In 1986, Clear Lake was added to the Clean Water Act Section 303(d) List of Impaired Water Bodies due to impairments from nutrients causing nuisance algal blooms and impacting multiple beneficial uses. As a result of the nutrient impairment listing, on June 23, 2006, the Central Valley Water Board adopted Resolution No. R5- 2006-0060, Amending the Water Quality Control Plan (Basin Plan) for the Sacramento and San Joaquin Rivers Basins for the Control of Nutrients in Clear Lake. USEPA approved the control program as a Total Maximum Daily Load (TMDL) on September 19, 2007. In the most recent Clean Water Act Section 303(d) List of Impaired Water Bodies from 2020-2022, a new listing for microcystins for Clear Lake has been proposed and approved by the State Water Resources Control Board and still requires approval from USEPA.

In recent years, Clear Lake has experienced a rise in cyanoHAB events and the associated impacts from these events. Cyanobacterial blooms occur throughout much of the year, characterized by planktonic and benthic cyanobacterial species capable of producing toxins. Multiple cyanotoxins have been documented in the lake, but their spatial and temporal distributions are poorly understood.

Clear Lake monitoring data and conventional wisdom from observers indicate that blooms may initiate as early as February in the upper, northwestern arm of the lake, and that surface-associated phytoplankton are often blown by the predominant northwesterly winds into the southeastern arms, where they can accumulate at tremendous concentrations. Due to the presence of substantial levels of cyanotoxins in Clear Lake, several groups have conducted, or are presently conducting, monitoring programs of water quality within the lake, including the Elem Indian Colony, the Big Valley Band of Pomo Indians, the California State Water Resources Control Board, and the California Department of Water Resources. These ongoing monitoring and observational programs conducted in the lake, along with published reports, document high cyanobacterial diversity including the following genera: *Anabaena, Aphanizomenon, Aphanocapsa, Chroococcus, Cylindrospermopsis, Dolichospermum, Geitlerinema, Gloeocapsa, Gloeotrichia, Woronichinia, Microcystis, Oscillatoria, Phormidium, Planktothrix,*

Pseudanabaena, and *Lyngbya.* Given the diversity of cyanobacterial genera in the lake, there is a potential for several cyanotoxins to be present including, but not exclusive to, microcystins, anatoxins, cylindrospermopsins, saxitoxins, and nodularin. To date, however, there is limited data characterizing cyanobacterial community composition and cyanotoxins with co-occurring measurements of environmental conditions. The lack of co-located (in space and time) environmental characterization along with cyanoHAB characterization has prevented an understanding of the specific environmental drivers of toxic events in Clear Lake.

The overall purpose of the Clear Lake Study was to identify the environmental drivers (i.e., lake chemistry and physics) leading to cyanobacterial bloom development and the production of cyanotoxins. Information on environmental drivers can be used by the Central Valley Water Board to support future consideration of water quality goals or other actions at Clear Lake, if warranted, and any subsequent actions needed to address the identified drivers.

METHODS

Study Site Description

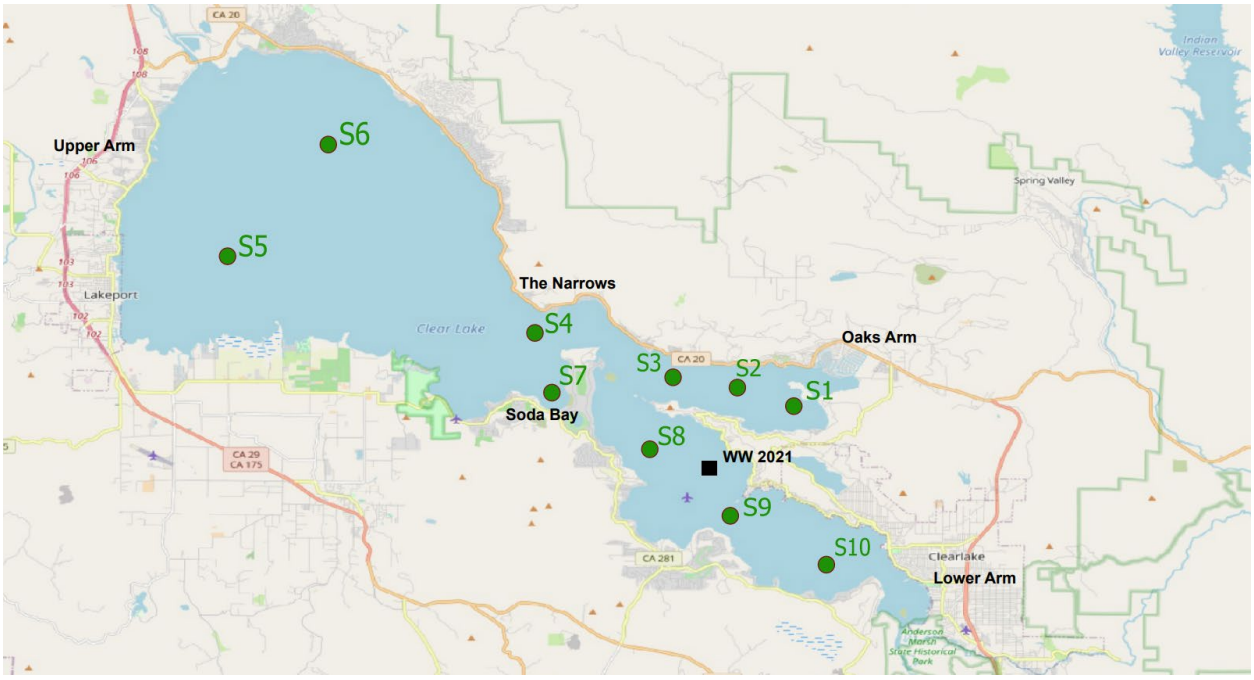

Figure 1. Map of Clear Lake sampling stations for 2020 and 2021 surveys, shown with green circles. In 2020, the WireWalker was deployed at station 4, while in 2021, the WireWalker was deployed between stations 8 and 9, indicated on the map with a black square.

A total of thirteen lake-wide surveys were conducted in 2020 and 2021 on Clear Lake to compare the biological and physio-chemical parameters that influence the extent, duration, and microcystin concentrations of cyanobacterial blooms. The 2020 survey focused on capturing cyanobacterial dynamics at a finer temporal scale through sampling approximately every 3-4 days during the month of August. The 2020 sampling plan was significantly affected by, and consequently adjusted, due to COVID-19. Boat surveys were conducted in 2020 on August 5, August 8, August 11, August 14, August 18, August 21, August 25, and August 28. The 2021

survey was purposely conducted at a coarser temporal scale, sampling the lake at approximately monthly intervals to capture cyanobacterial dynamics in the lake across much of the bloom season. Surveys in 2021 were conducted on June 17, July 13, August 10, September 20, and October 28. Both survey years consisted of ten sampling stations per visitation, distributed amongst the three arms of the lake (Figure 1, Table 1). All sampling stations were conducted in open water (i.e., away from the immediate proximity of the shore).

Table 1. Geographic coordinates of sampling stations.

Station ID	Lake Arm	Latitude	Longitude
Station 1	Oaks	39°0.352'	-122°41.137'
Station 2	Oaks	39°0.747'	-122°42.347'
Station 3	Oaks	39°0.881'	-122°43.455'
Station 4 (WireWalker 2020)	Upper (The Narrows)	39°1.767'	-122°46.092'
Station 5	Upper	39°3.410'	-122°51.746'
Station 6	Upper	39°5.405'	-122°50.067'
Station 7	Upper (Soda Bay)	39°0.593'	-122°45.871'
Station 8	Lower	38°59.703'	-122°43.780'
Station 9	Lower	38°58.234'	-122°42.349'
Station 10	Lower	38°57.582'	-122°40.353'
WireWalker 2021	Lower	38°59.100'	-122°42.775'

Discrete Sample collection

Whole (i.e., unfiltered) water samples were collected at each sampling location using a clean plastic bucket at or near the water surface. Plankton net tow samples (20 µm mesh) were also collected at each station by lowering and raising the net 1-3 times (surface to ≈2 m). All collection bottles were rinsed three times with sample water before filling. Filled bottles were kept cool and dark while in the field. Additional processing of water samples was conducted at an onsite field laboratory within 12 hours of sample collection. Whole water samples were used for nutrients, cyanotoxins, chlorophyll a, Lugol's and formaldehyde preserved algal samples, and molecular analyses. Net tow samples were preserved with formalin for later microscopical analysis to assess community composition. For each station, the collector logged the collection of each sample type into a field sheet that has been retained. Photographs of notable surface algae were taken and saved in a digital repository. Nutrient, cyanotoxin, and chlorophyll a samples were frozen in the field and later stored at -20°C upon return to the lab. Molecular samples were flash frozen in liquid nitrogen and stored long term at -80°C. Preserved samples were kept at 4°C in the field and upon return to the lab.

Vertical profiles of water temperature, dissolved oxygen (DO), pH, and conductivity were conducted at each station using an RBR Concerto (https://rbr-global.com/). Operation and maintenance of water quality meters followed the manufacturer's recommendations. Profiles were successfully collected at most stations each year, with the exception of the survey conducted in October 2021, where the instrument failed.

Discrete Laboratory Analyses

Chlorophyll a

25mL of whole water for chlorophyll *a* (chl *a*) analysis were concentrated via gentle filtration onto glass fiber filters (Sterlitech, grade F, Kent, WA). Filters were extracted in 100% acetone at -20°C in the dark for 24 hours to ensure thorough extraction. Sample extracts were analyzed fluorometrically via the non-acidification method using a Trilogy Turner Designs fluorometer (Turner Designs, Sunnyvale, CA). Duplicate filters were collected at all stations and the average chlorophyll *a* concentration of the two filters is reported here.

Microcystins analyses from Water Samples

For the analysis of total microcystins, samples were lysed via a freeze-thaw cycle three times to ensure cell disruption. The extract was then filtered and analyzed according to the manufacturer's instructions. Samples for dissolved toxins were collected after filtration through a 0.2 µm syringe filter. Samples with concentrations higher than the standard curve were serially diluted with kit-provided dilution buffer until sample concentration was within the working range of the kit.

In 2020, both the particulate and total toxin samples were analyzed via ADDA ELISA test kits (Abraxis, Part No. 520011, Warminster, PA). The assay detects all microcystin and nodularin variants with the ADDA side group in bulk and does not provide data for specific congeners of the toxin class. Dissolved toxin values were derived by subtracting particulate microcystins from total microcystins. In 2021, dissolved and total toxin samples were analyzed using the ELISA kits and particulate microcystins were derived by subtracting dissolved microcystin concentrations from total microcystin concentrations.

Microcystins analyses from Passive Samplers

SPATT bags were constructed with Diaion HP20 resin (Sorbtech; Norcross, GA) and 100 µm mesh (Wildco; Yulee, FL) and supported by an embroidery hoop ring. After construction, the bags were activated in 100% MeOH at 4°C for 24 hours, then rinsed and stored in ultrapure water at 4°C until use as described in Lane et al. (2010). SPATT were deployed to monitor for cyanotoxins at one location in the lake each year. SPATT was deployed in August of 2020 (39°1.767', 122°46.092') and in June, July, and August of 2021 (38°59.100'N, 122°42.775'W). SPATT samplers were not analyzed under the current funding phase and were archived for future analysis.

Nutrients

Total nitrogen and total phosphorus samples were collected by aliquoting whole water into a single 60 mL HDPE jar for analyses. Samples were kept on ice, and frozen at -20°C immediately upon return to the lab. Samples were analyzed colorimetrically following EPA Methods 353.2 for total nitrogen and 365.1 for total phosphorus at the University of Maryland Center for Environmental Science Nutrient Analytical Services Laboratory.

Nucleic Acid Extraction

Nucleic acids (DNA and RNA) were extracted using the Qiagen DNEasy PowerBiofilm Kit. Cyanobacteria from Clear Lake are difficult to extract using the kit alone because of high biomass and the nature of many of samples that were dominated by colonial cyanobacteria, their associated mucilage, and difficulty in breaking open cells. Several protocol optimization experiments resulted in the addition of a few steps to the Qiagen protocol. The first two Qiagen solutions are added to the samples as the protocol states. The samples were then rapidly freeze-thawed in liquid nitrogen to enhance lysing of cells. 25 µL of proteinase K was then added to each sample and incubated at 55°C for a minimum of four hours or overnight. After the proteinase K incubation, the Qiagen kit protocol was followed according to the manufacturer's instructions. Extracted nucleic acids were quantified with NanoDrop UV-Vis spectroscopy and Qubit Spectrofluorometry. The NanoDrop was be used to determine nucleic acid quality by confirming a 260/280 ratio between 1.8 and 2. DNA samples from 2020 were sent to Novogene (Nanjing, China) for library preparation and 25 Gbp of Illumina PE 150bp sequencing. DNA samples for 2021 were sent to the Norris Cancer Center Genome Core at USC for library prep and sequencing of the same parameters.

Samples to be investigated for prokaryote and microbial eukaryote species richness and community composition were examined through tag sequencing (sequencing of the V4 hypervariable region of small subunit rRNA genes; 16S and 18S). Samples were processed according to the general protocol for nucleic acid extraction noted above. The V4 region was amplified using universal primers that were designed to amplify all three domains of life (Yeh et al. 2021).

Statistical Analyses

Metagenomic Assembly and Analysis

After receiving raw metagenomic reads from the sequencing center, the paired end reads were examined for quality using FastQC v0.11.5 (Andrews 2010). If the FastQC results indicated a need for trimming, the reads were trimmed using Trimmomatic v0.36 (Bolger et al. 2014). De novo genome assembly was done using MetaSPAdes v3.13.0 (Nurk et al. 2017), MEGAHIT (Li et al. 2015), and IDBA-UD (Peng et al. 2012). The highest quality resulting assembly (based on a combination of contig length, N50, and contig number) was used for downstream processing. An initial clustering of contigs was done using CONCOCT (Alneberg et al. 2013). Metagenome assembled genomes (MAGs) were then binned by hand using the program Anvi'o (Eren et al. 2020, 2021).

Raw metagenomic reads were fed into the program PhyloFlash (Gruber-Vodicka et al. 2020) to extract 16S and 18S rRNA reads which were then used to determine the community composition of each sample, and compare against targeted tag sequencing of V4 hypervariable regions of 16S and 18S genes to document microbial species richness and community composition. MAGs were also used to determine the composition of the cyanobacterial community. All sequences will be publicly available via the NCBI Sequence Read Archive (Leinonen et al. 2011).

Statistical Associations between HAB indicators and Environmental Parameters

Temperature, dissolved oxygen, total nitrogen, total phosphorus chlorophyll *a*, and total, particulate, and dissolved microcystins concentrations were organized into data sets that were

categorized by all data and data by year. Spearman rank order correlation analysis was used to determine the strength of association between total microcystins, particulate microcystins and dissolved microcystins with environmental variables. A significant correlation was defined as variables with a positive or negative Spearman's correlation coefficient (ρ) with a $p < 0.05$. These analyses were conducted using the "Hmisc" package in R.

Instrumented Measures

WireWalker

A WireWalker vertical profiler (Rainville & Pinkel 2001; Pinkel et al. 2011) was moored at Station 4 (39°1.767', 122°46.092') in 2020 and between Stations 8 and 9 (38°59.100'N, 122°42.775'W) in 2021 during the study (Figure 1). The WireWalker is a profiling platform that uses wave energy to gain downward motion of a positively buoyant instrument along a moored wire. The instrument rachets down the wire to a fixed depth where a trigger releases it from the ratcheting mechanism to allow it to float up the wire to the surface where it reengages the rachet. The WireWalker is an "instrument mule" that carries sensors up and down the wire, providing continuous vertical profiling of pertinent environmental variables, as determined by the attached sensor packages. The WireWalker was outfitted with a RBR Concerto that simultaneously measured depth, temperature, conductivity, dissolved oxygen, and chlorophyll *a* fluorescence. In 2020, the RBR sampled at a rate of 2Hz. The sensor package near Station 4 collected profiles from 0.3-5.2 m in 2020. Data were collected from August 3-28 in 2020, with a total of 17,777 profiles collected. The sensor package near Station 8 collected profiles from 0.5-7.3 m in 2021. The RBR sampled at a rate of 2Hz, and data were collected from June 16 until August 11 in 2021, after which time the instrument package malfunctioned (September) and then the platform was subsequently lost due to parting of the wire between the time the instrument was deployed in September and attempted recovery in October. A total of 25,754 profiles were collected prior to instrument failure and loss.

EcoMapper

We collaborated with Xylem Environmental Solutions to use their YSI i3XO EcoMapper, an underwater autonomous vehicle (AUV) to profile Clear Lake. The EcoMapper is a powered AUV that, similar to the WireWalker, carries a variety of sensors that record continuously as the instrument moves along a pre-programmed mission line. For its missions in Clear Lake, the EcoMapper carried sensors to measure depth, temperature, conductivity, dissolved oxygen, chlorophyll *a* fluorescence and phycocyanin fluorescence ("Total Algae"), and pH. For the whole-lake transects conducted in each arm of the lake, the instrument flew along a horizontal track while it continuously rose or sank (a "yo-yo" pattern) between near-surface and near-bottom depths as it moved forward. The resulting sensed data were then contoured to provide two-dimensional depictions (horizontal run vs depth) of each sensed parameter along the transect line. One mission was also conducted in Konocti Bay of Lower Arm to examine small-scale spatial heterogeneity at one depth (1.5 m). The criss-cross (lawnmower) pattern deployment allowed the construction of two-dimensional contour plots of each sensed parameter.

In 2020, the instrument was used to profile three transects along the main axis of each of the lake's arms (Figure 2A) during the period of the August visitation. In June 2021, the EcoMapper again profiled a single transect in each arm of the lake, as well as the higher spatial resolution grid pattern in Konocti Bay of Lower Arm (Figure 2B). In October 2021, only the transect of the Upper Arm was collected because floating debris from a recent severe storm presented a significant navigation hazard for the instrument.

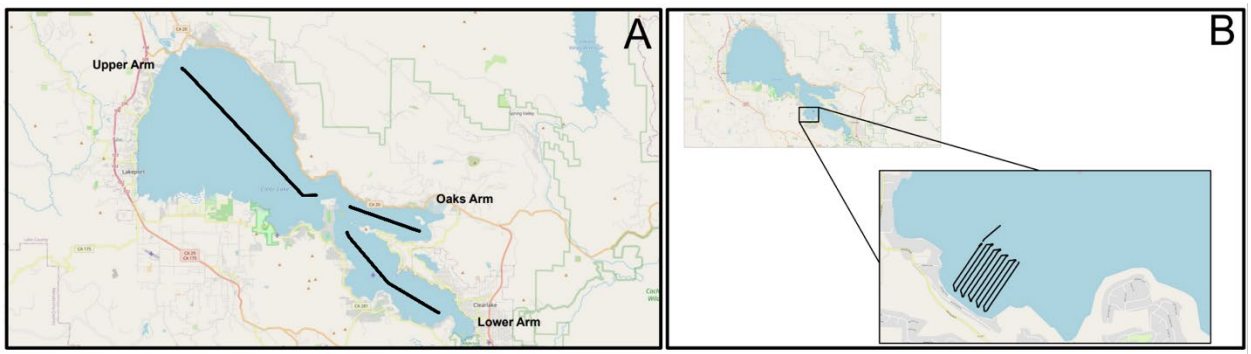

Figure 2. Map of Clear Lake EcoMapper transects in 2020 and 2021. A: Transects in each arm of the lake. B: Higher resolution transect of Konocti Bay in the Lower Arm.

Drone

A small Unmanned Aerial System (sUAS; a hyperspectral drone; DJI Matrice 200 V2 Drone System; DJI Enterprise) was deployed as a part of the study of small-scale spatial heterogeneity of cyanobacterial abundances in Konocti Bay (see next section). The sUAS is a four-prop instrument that carries four sensor payloads:

Sensor 1: 3 Channel Sensor

Blue: 446 nm CWL x 60 nm width

Green: 548 nm CWL x 45 nm width

Red: 650 nm CWL x 70 nm width

Sensor 2: Single Channel Sensor

UV: 400 nm CWL x 25 nm width

Sensor 3: Single Channel Sensor

Red / Red Edge: 700 nm CWL x 25 nm width

Sensor 4: Single Channel Sensor

Red Edge: 725 nm CWL x 25 nm width

Overflights of the instrument within Konocti Bay were used to map the spatial heterogeneity of cyanobacterial/algal accumulations at the lake surface during the August 2020 deployment. Photographic images of scums formed by wind-blown, buoyant cyanobacteria were captured by

the drone imagery, and used to compare to sensed parameters observed by the EcoMapper at 1.5 m depth, and to discrete samples collected from a boat at the surface of the lake and at 1.5 m throughout the study area.

Whole lake and small-scale spatial heterogeneity surveys

The automated sensor-equipped instrumentation (the WireWalker, the EcoMapper, and the drone) were deployed in Clear Lake in two manners.

Whole-lake surveys: The WireWalker and EcoMapper were deployed during 2020 and 2021 to obtain synoptic spatial and temporal observational information for the lake. As noted above, the EcoMapper conducted missions along the main axes of the three arms of the lake (all three arms were examined in August), while only the Upper Arm mission could be conducted in 2021 (Figure 2A) because of floating obstacles introduced by heavy rains prior to the October visitation, which posed an entangled issue. Preliminary data analysis and contouring have been performed on the 2020 EcoMapper data and are discussed below. The WireWalker was deployed in Lower Arm during 2021, in order to capture chemical physical data for an arm of the lake that often experiences intense cyanobacterial blooms and toxin concentrations (WW 2021 station in Figure 1). The WireWalker was deployed for the entire month-long visitation of the lake in August 2020 at a location near the confluence of the three arms of the lake (approximate to station 4 in Figure 1). The deployment location, near the southwestern end of Upper Arm, is near the overall "center" of the lake and generally experiences considerable wave action due to the significant wind fetch along the axis of Upper Arm. The location therefore captures the overall pattern and magnitude of wind forcing on the lake surface, providing an index of wind-induced mixing.

Survey of small-scale spatial heterogeneity of a cyanobacterial bloom: The purpose of this survey was to establish how decision regarding where and how to sample a cyanobacterial bloom can affect the resulting information obtained about the bloom. Heterogeneous distributions of cyanobacterial cells resulting from surface and/or subsurface preferences of a species, as well as wind accumulation, pose important considerations when obtaining and interpreting samples for HAB analysis. This study was conducted to document these small-scale distributions and the range of outcomes in assessing blooms that relate to the mode and approach employed in characterizing and sampling a bloom. To accomplish this task, the EcoMapper and drone were deployed in conjunction with a program of discrete sampling from a boat in Konocti Bay in order to document the impact of a patchy distribution of cyanobacterial cells on bloom magnitude and toxin concentrations in the resulting samples. Sampling from a boat was conducted at two depths, surface and 1.5 m at 10 stations across the sampling area. Accurate sampling at 1.5 m depth was accomplished using a Niskin bottle sampler with the openings at either end of the sampler oriented horizontally on the downline. Surface water samples were collected by hand in 100 ml amber bottles from visible aggregations of cyanobacteria (surface clumps and scums) and from locations immediate nearby but without visible aggregations. The EcoMapper was deployed along a lawnmower pattern throughout the sampling area at a constant depth of 1.5 m, in order to collect sensor data (as described previously) at the same depth as the Niskin bottle sampling. The EcoMapper also collected bottom depth during the study. The drone was flown above the study area during the time or EcoMapper flight and discrete water sampling. Imagery is still being processed at this time but will be made available upon completion of analysis. Representative images are presented and discussed below.

RESULTS AND DISCUSSION

Discrete Sampling

Chlorophyll a Concentrations and Microscopy Based Community Composition

Chlorophyll *a* concentrations (a proxy for overall algal biomass) ranged from 12.68 to 149.31 µg/L during the August 2020 survey period (Figure 3A). Overall, the spatial patterns remained somewhat consistent when compared across the stations, although the absolute concentrations were different in the three arms of the lake (Figure 3B). Chlorophyll *a* concentrations increased early in the month between August 5-8, 2020. A lake-wide decline in concentrations were observed on August 11, 2020, indicating a decline in overall algal biomass. This decline in concentrations continued at most stations between August 11-13, 2020. Concentrations of chlorophyll *a* then increased at all stations between August 14-24, 2020, with many stations at similar or higher concentrations than previously observed peak on August 8, 2020. Overall, the results indicate the presence of a waning bloom in early August at the onset of our study in 2020, followed by another bloom appearing late in the month.

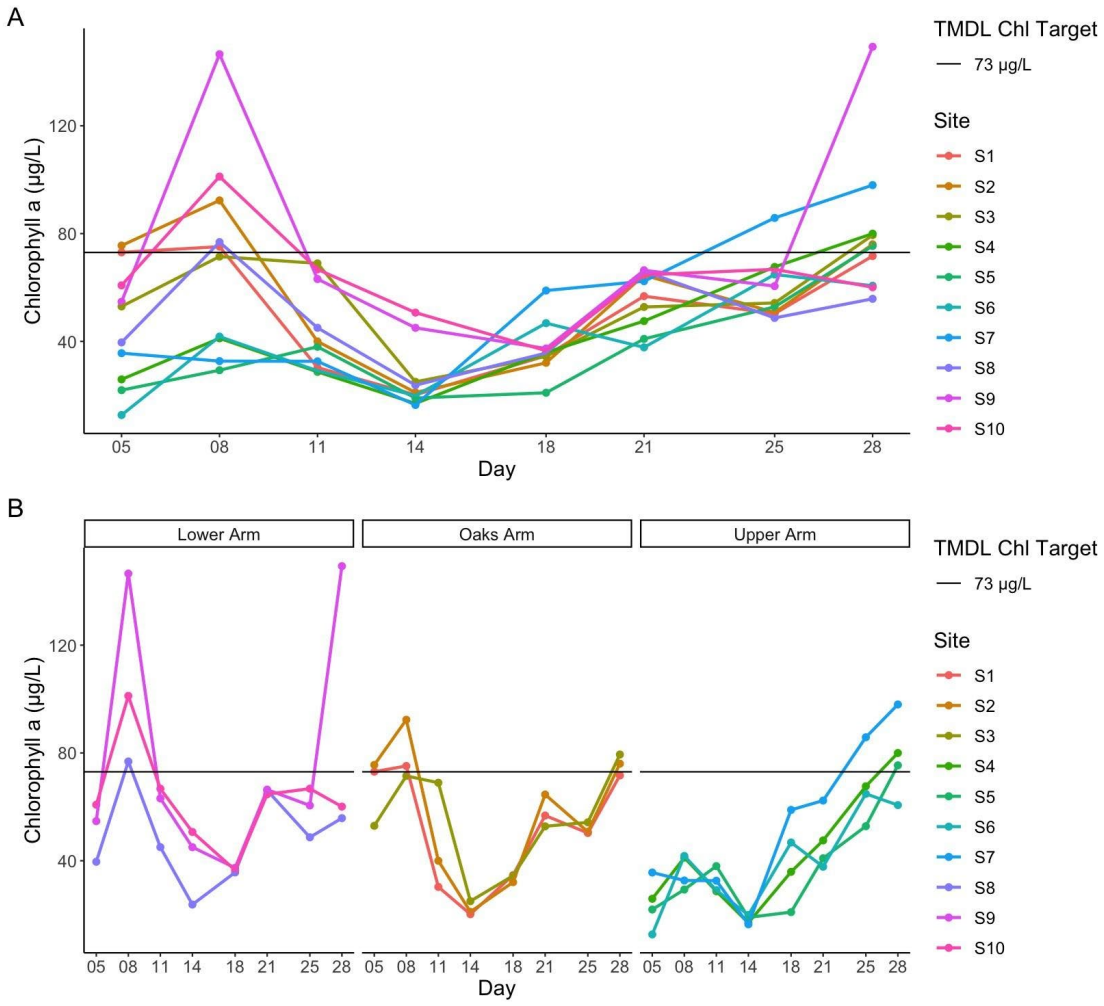

Figure 3. Chlorophyll a concentrations observed in Clear Lake during the August 2020 survey plotted by all stations (A) and faceted by each lake lobe (B).

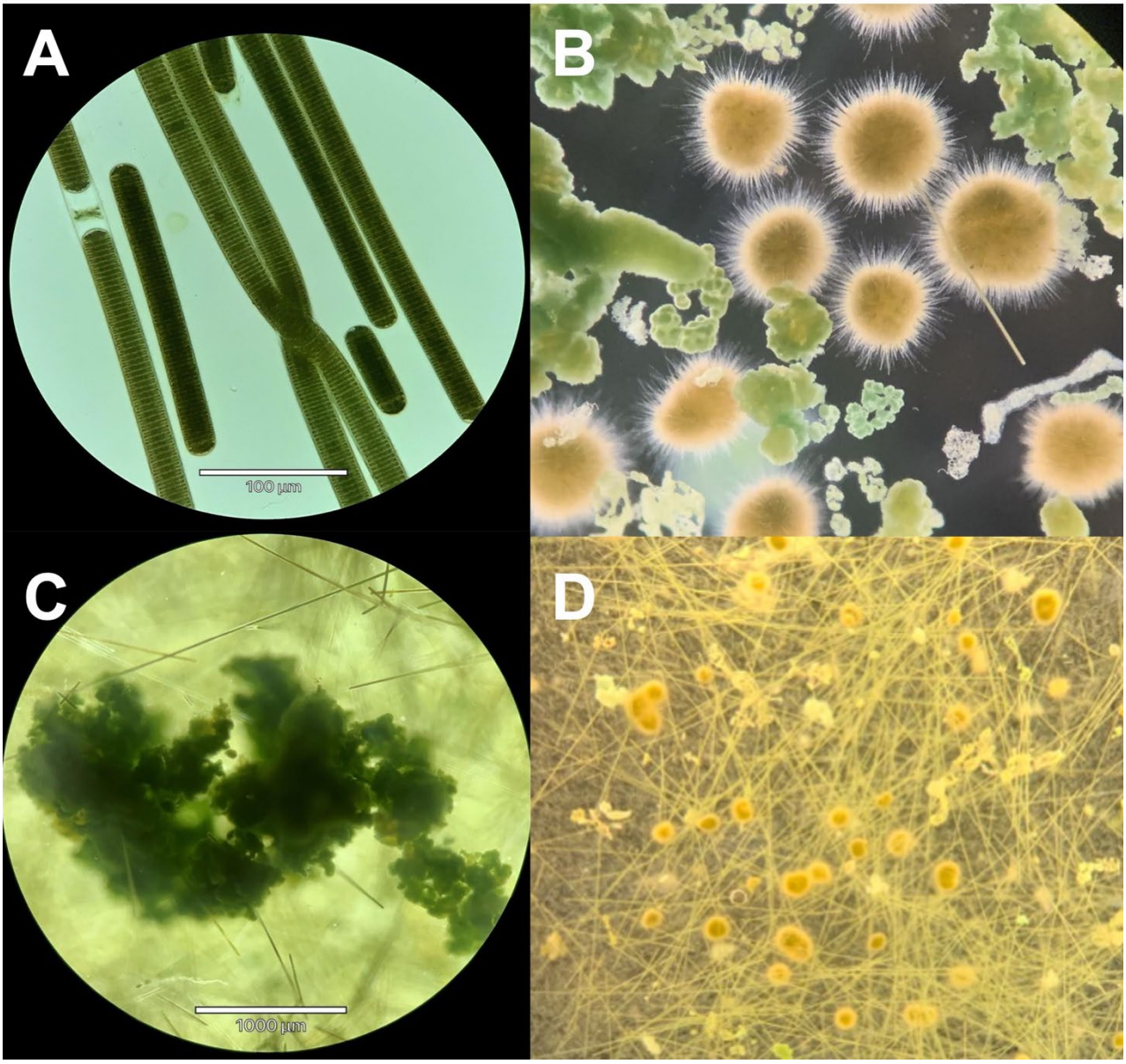

Figure 4. Micrographs of key cyanobacterial taxa observed in Clear Lake during the 2020 and 2021 field surveys. Lyngbya spp. (A), Gleotrichia spp. (B), Microcystis spp. (C) and a mixed community of Lyngbya spp. Gleotrichia spp. observed in June 2021 (D).

Qualitative microscopic observations of sample water showed that the cyanobacterial community was largely dominated by *Lyngbya spp.* (Figure 4A,D) for most of August 2020, though several other toxigenic taxa were also observed throughout the month. *Gleotrichia spp* (Figure 4B). was observed during the first week of observations, particularly at Station 4 and Station 7. *Microcystis spp* (Figure 4C). were also commonly observed throughout August, particularly at stations within the Lower and Oaks Arms.

During the five monthly visitations to Clear Lake in 2021, chlorophyll *a* concentrations ranged from 17.10 µg/L to 736.74 µg/L (Figure 5A). The large amount of variability that occurred in chlorophyll concentrations observed across the five months occurred over space as well as time.

As in 2020, the Lower and Oaks Arms generally exhibited higher surface water concentrations of chlorophyll *a* than the stations in the Upper Arm. The timing of the highest concentrations in each arm varied somewhat, with maximal concentrations in the Upper Arm observed during August (Station 6) and September (Stations 4, 5, and 7) surveys across all stations. The Lower Arm had maximal chlorophyll concentrations at all stations in September, while the Oaks Arm had its highest concentration in July at Station 3, followed by high concentrations at Station 1 and Station 2 in August (Figure 5B).

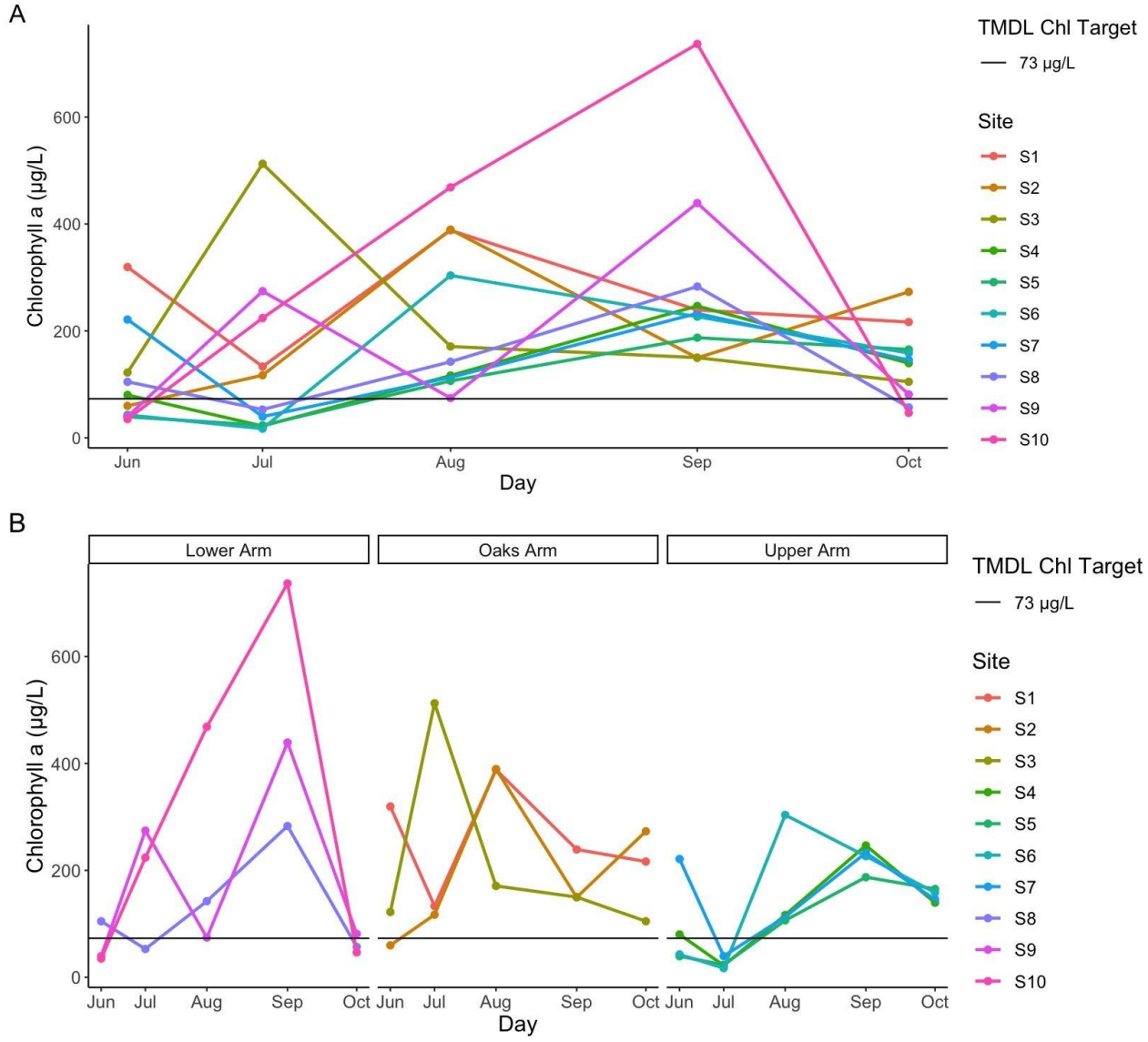

Figure 5. Chlorophyll a concentrations observed in Clear Lake during the August 2021 survey plotted across all stations (A) and faceted by each lake lobe (B).

In 2021, microscopic observations of sample water showed several shifts in cyanobacterial community composition between June and October. In June 2021, *Gloeotrichia spp.* (Figure 4B, D) was a dominant member of the community throughout the lake. As in August 2020, *Lyngba spp.* (Figure 4A) was also a common member of the cyanobacterial community in June 2021 and

was co-dominant with *Gloeotrichia spp.,* in the Lower and Oaks Arms (Figure 4D). During the following visit in July 2021, community dominance in the lake shifted to *Microcystis spp.* (Figure 4C), though *Gloeotrichia spp.* was still commonly observed. Later in August 2021, the community was almost entirely dominated by *Microcystis spp*. Overall cyanobacterial abundances decreased in September 2021 in the Upper Arm, though *Microcystis spp*. remained dominant in the Lower and Oaks Arms. Community composition patterns generally remained similar in October 2021, though overall biomass dropped from the previous month.
A target chlorophyll *a* concentration of 73 µg/L was established in the 2007 TMDL. During the 2020 August survey, multiple observations of concentrations above that target were observed. A total of 18% of samples collected were greater than that concentration and most of those observations were collected in the Lower and Oaks Arms (Figure 3B). Exceedances of the TMDL chlorophyll *a* target were also observed across multiple months in 2021. Concentrations of chlorophyll *a* exceeded the TMDL target in 76% of samples collected, with at least one station exceeding this target each survey month (Figure 5B).

Temporal and Spatial Dynamics of Microcystins

All ten sampling stations were positive for total microcystins at least once during the month of August 2020 (Figure 6, Figure 7A). Temporally, total microcystin concentrations were highest in the first two surveys near the beginning of August. The highest concentration of total microcystins was 5.08 µg/L which occurred at Station 8 on August 8, 2020. This maximal value at Station 8 corresponded with peaks at several other stations, particularly in the Lower and Oaks Arms. Following the observations on August 8, 2020, there was an overall dip in total microcystin concentrations lake wide (Figure 6, Figure 7), though toxin was detected at most stations. At the end of the sampling period (August 28, 2020), all ten stations were positive for total microcystins, though most were less than 1 µg/L. Over the last two sampling events, a precipitous rise in total microcystin concentrations was also observed in stations 9 and 10 located in Lower Arm. Overall, the Warning threshold (0.8 µg/L) was exceeded a total of 19 times during the month of August, all of which occurred in the Lower and Oaks Arms of the lake. The Upper Arm of the lake was consistently lower in microcystin concentrations than the Oaks and Lower Arms (Figure 7B).

Across all stations, the overall partitioning of microcystins between the particulate and dissolved pools varied across stations and time (Table 2). At most stations, the concentration of toxin in the particulate pool comprised the smaller fraction of the total toxin pool, with the overall percentage of detectable toxin present in the dissolved fraction ranging from 73% to 97% of the total pool. Conversely, the particulate fraction generally made up a smaller fraction of the total pool with the contribution to the total pool ranging between 2% and 27%.

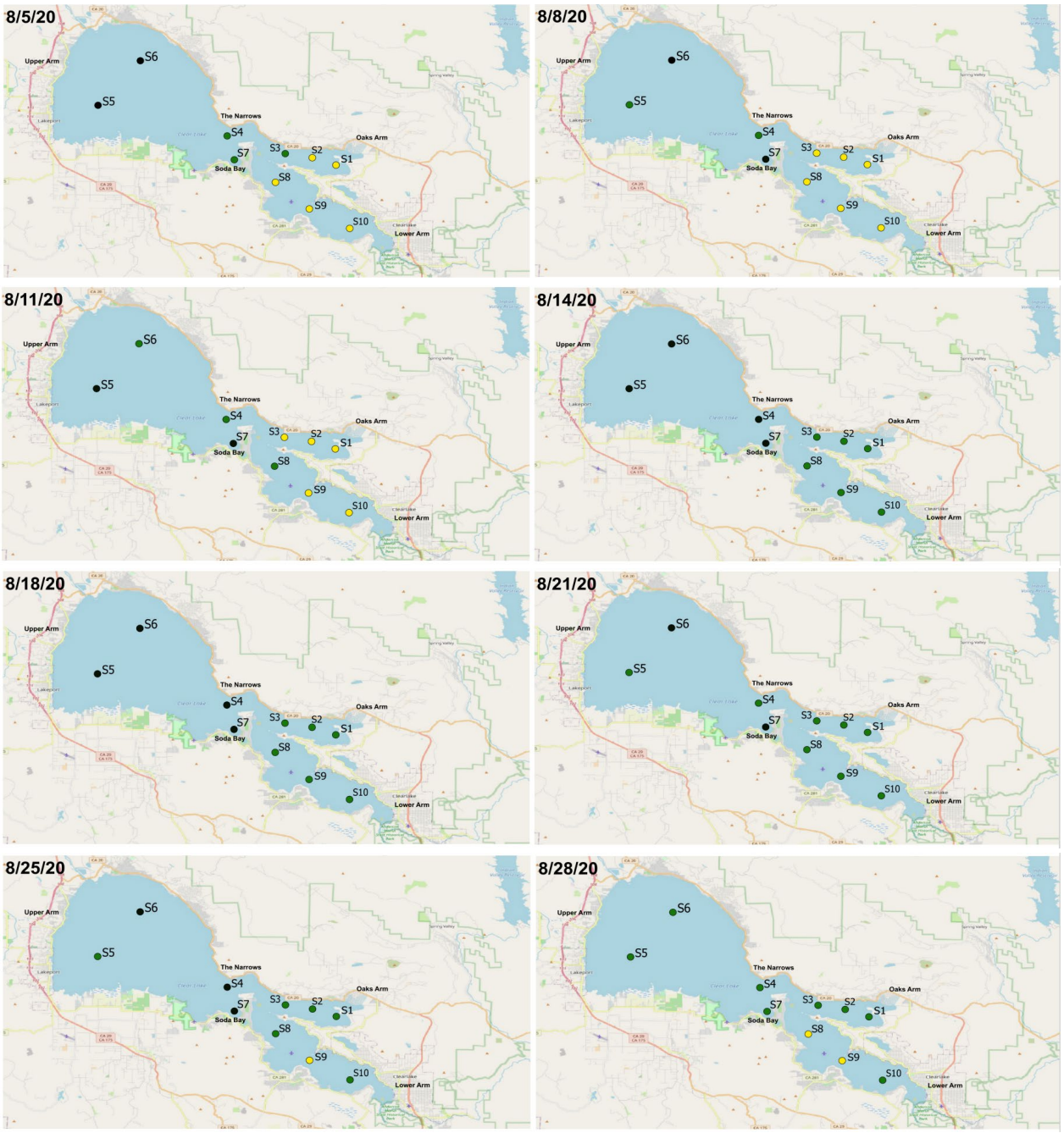

Figure 6. Changes in spatial distribution of total microcystin concentrations in Clear Lake during the 2020 sampling season. Black points indicate where no microcystins were detected. Green points indicate that microcystins were detected but below any trigger level. Yellow points indicate stations that were above the California State Caution level, orange points indicate stations that were above the California State Warning level, and red points indicate stations that were above the California State Danger level for microcystins.

Table 2. Range of concentrations of Total Microcystins, Particulate Microcystins and Dissolved Microcystins observed at each station during August 2020 and June-October 2021.

2020			
Station	Total Microcystins (µg/L)	Particulate Microcystins (µg/L)	Dissolved Microcystins (µg/L)
Station 1	0.23-2.38	0.009-0.249	0.22-2.20
Station 2	0.19-1.91	0.028-0.382	0.15-1.60
Station 3	0.21-1.67	0.012-0.169	0.17-1.50
Station 4	bd-0.71	0.003-0.042	bd-0.71
Station 5	bd-0.34	0.003-0.074	bd-0.27
Station 6	bd-0.25	0.006-0.055	bd-0.197
Station 7	bd-0.25	bd-0.054	bd-0.20
Station 8	0.31-5.08	0.019-0.965	0.29-4.12
Station 9	0.44-3.56	0.044-0.386	0.39-3.17
Station 10	0.48-3.38	0.063-0.203	0.42-3.19
2021			
Station 1	0.53-4.2	0.31-3.92	bd-0.3
Station 2	0.75-8.44	0.75-8.21	bd-0.35
Station 3	1.73-3.86	1.38-3.67	bd-0.39
Station 4	bd-1.29	bd-1.29	bd-0.21
Station 5	bd-0.41	bd-0.35	bd-0.21
Station 6	bd-1.41	bd-1.41	bd-0.19
Station 7	bd-4.20	bd-4.2	bd-0.21
Station 8	0.98-74	0.98-73.5	bd-0.68
Station 9	2.3-62.5	2.3-61.9	bd-0.83
Station 10	1.6-190	1.37-188.6	bd-1.36

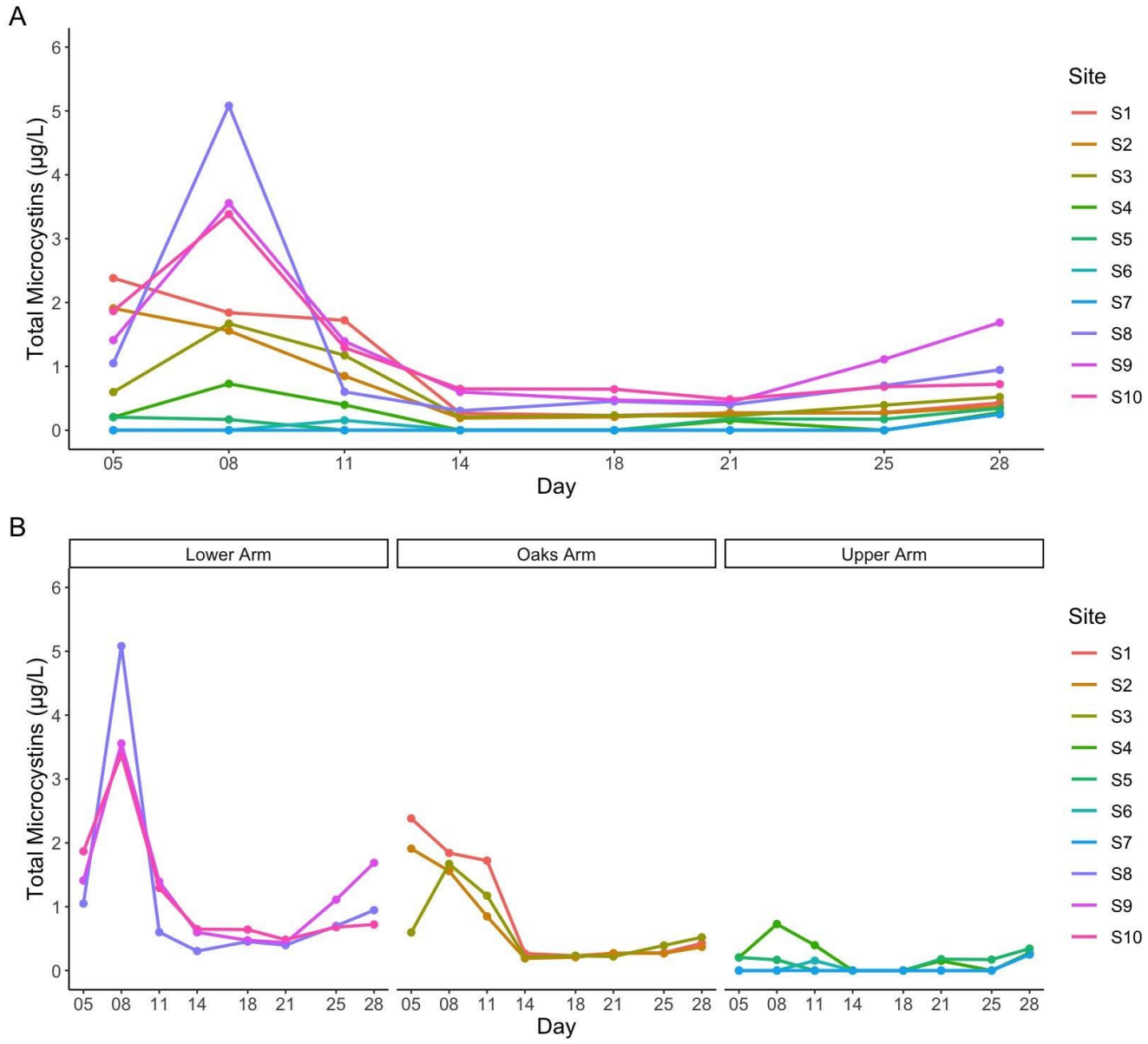

Figure 7. Total microcystin concentrations observed in Clear Lake during the August 2020 survey plotted across all stations (A) and faceted by each lake lobe (B).

Similar to 2021, all ten stations were positive for total microcystins at least once during the sampling period (Figure 8, Figure 9A). In August, September, and October, all stations were positive for total microcystins. The highest total microcystin concentration was 190.0 µg/L at Station 10 on September 9, 2021, exceeding the State of California Danger limit (Tier 3; 20 µg/L). Microcystin concentrations exceeded 20 µg/L a total of four times during the sampling period, concentrated during August and September, and all occurred in the Lower Arm of the lake (Stations 8, 9, and 10). The Warning threshold (Tier 2; 8 µg/L) was exceeded a total of eight times and the Caution threshold (Tier 1; 0.8 µg/L) was exceeded 18 times during the sampling period. The Upper Lake was noticeably less toxic than the Oaks and Lower Arms. No samples taken from the Upper Lake ever exceeded the Tier 1 threshold level (Figure 8, Figure 9B).

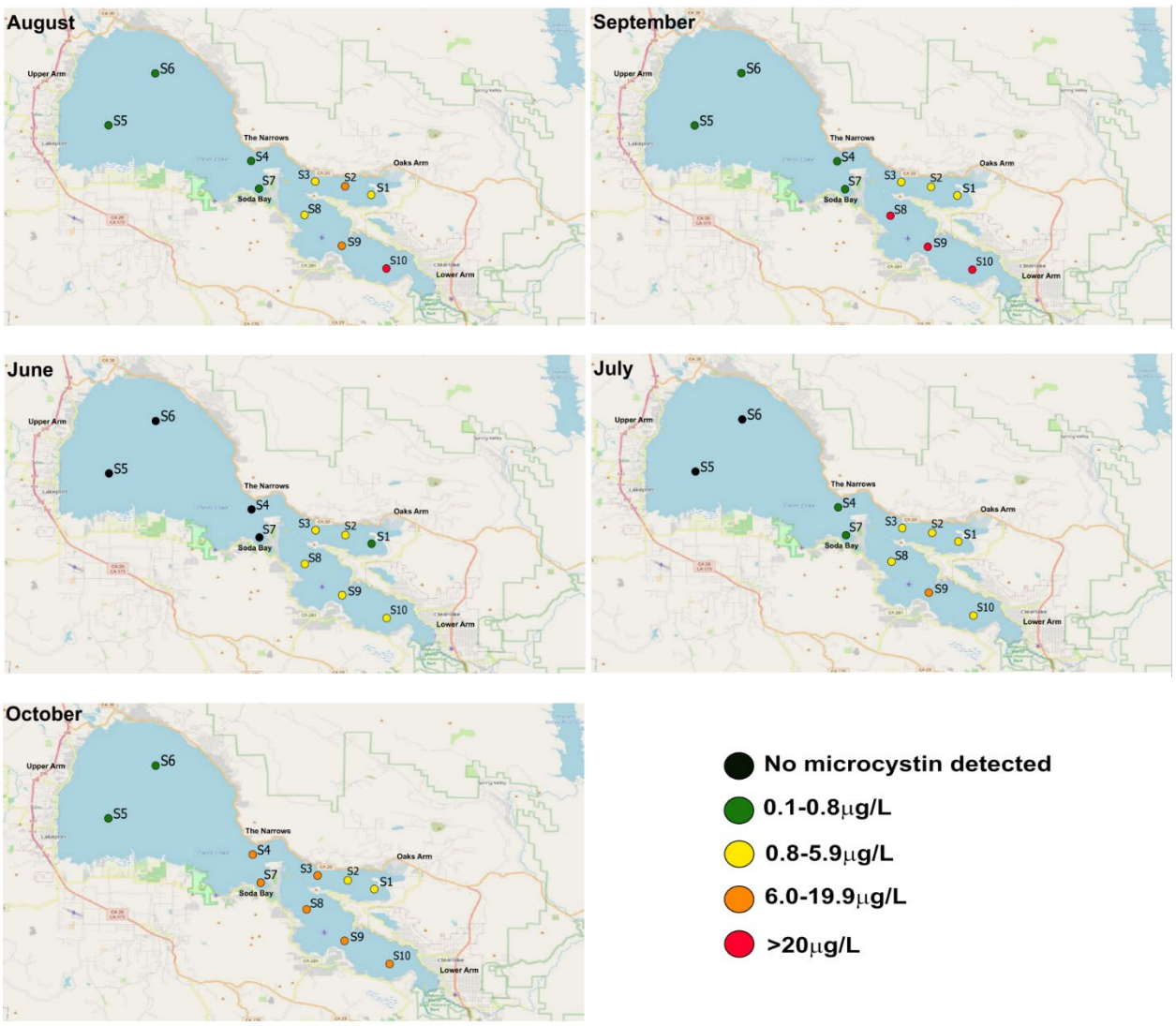

Figure 8. Changes in spatial distribution of total microcystin hits in Clear Lake during the 2021 sampling season. Black points indicate where no microcystins were detected. Green points indicate that microcystins were detected but below any trigger level. Yellow points indicate stations that were above the California State Caution level, orange points indicate stations that were above the California State Warning level, and red points indicate stations that were above the California State Danger level for microcystins.

Overall, August of 2020 had lower observed toxin concentrations than August of 2021 (for samples collected in 2020, and on August 11, 2021). The same date in 2020 did not have any stations that exceeded the Caution threshold, unlike in 2021 where two stations exceeded the Caution threshold and one station exceeded the Danger threshold (Figure 7A, 9A).

The partitioning of microcystins between the particulate and dissolved pools also varied more in 2021 than in August 2020, as might be expected given the greater temporal coverage in 2021 (Table 2). At most stations, particularly in the later months of the 2021 surveys, the concentration of toxin in the particulate pool comprised the larger fraction of the total toxin pool. A wider range of particulate pool contributions was observed with the overall percentage of detectable toxin present in the particulate fraction ranging from 22% to 100% of the total pool. During some months, dissolved toxin contributed significantly to the total pool, but the overall contributions ranged from 0% to 78%, showing more variance than in August 2020.

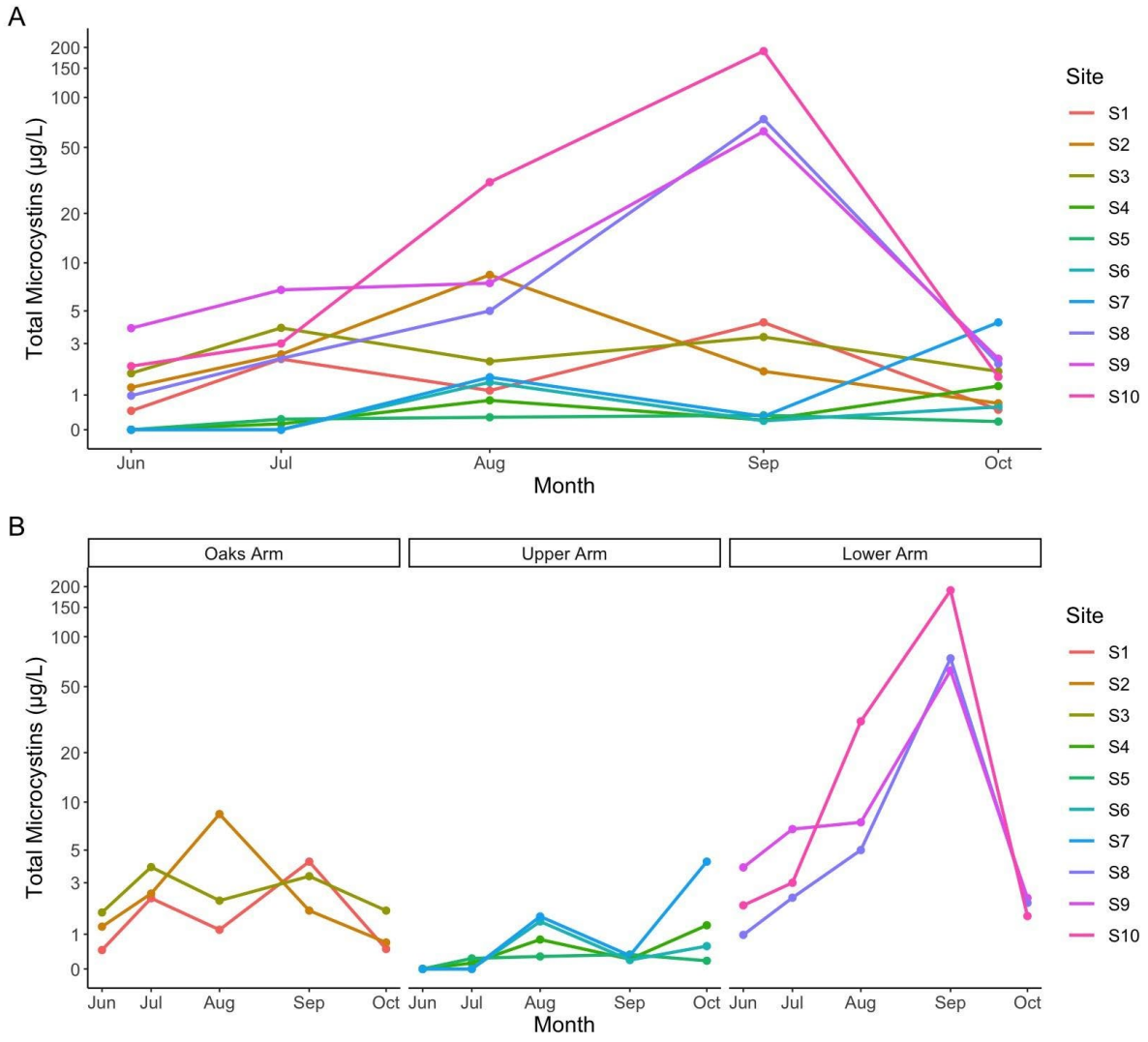

Figure 9. Total microcystin concentrations observed in Clear Lake during the August 2021 survey plotted across all stations (A) and faceted by each lake lobe (B).

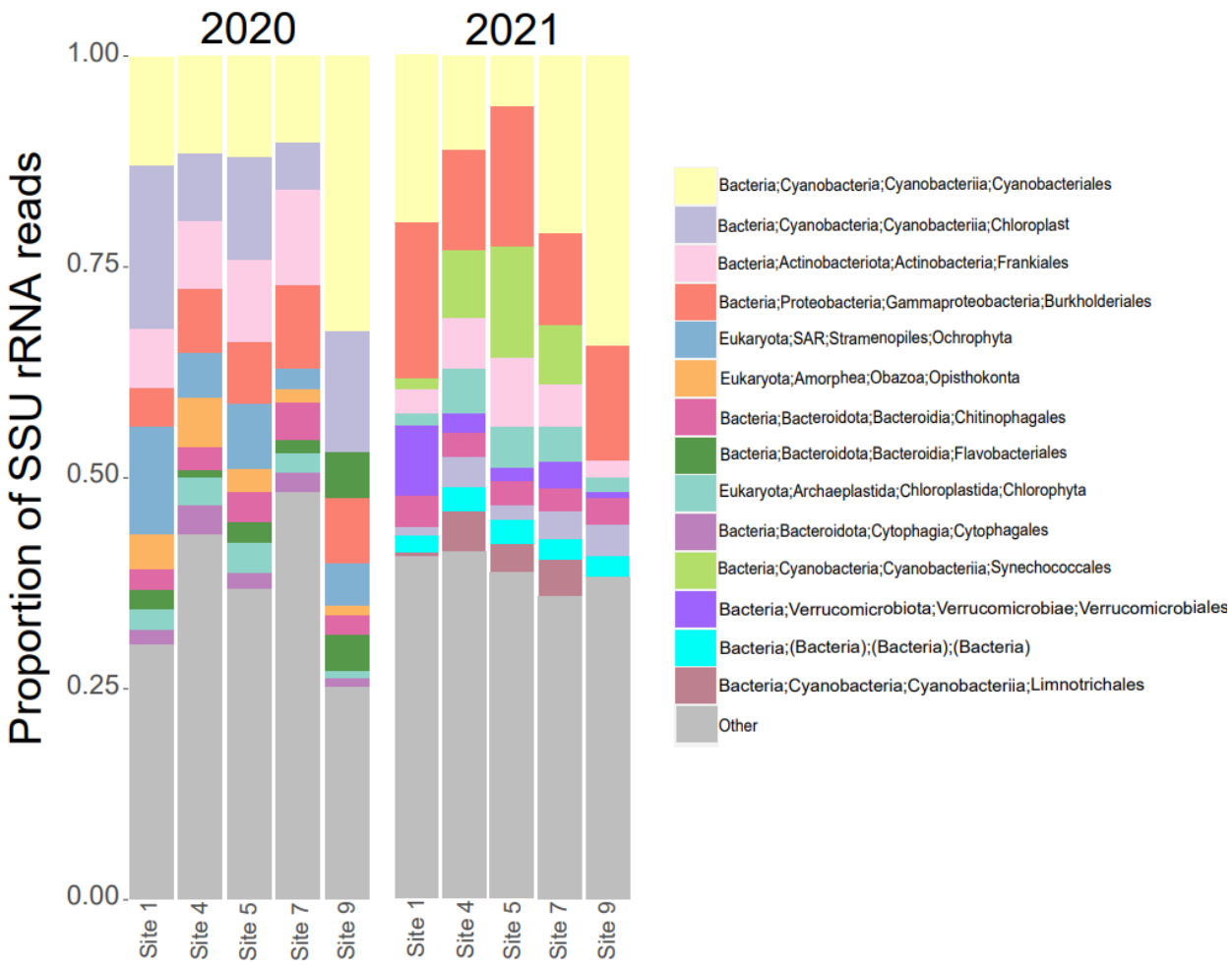

Figure 10. Relative abundance of small subunit (SSU) rRNA reads from each station in August of 2020 and 2021. Note that the yellow bars do not represent cyanobacteria, they represent chloroplasts from multiple taxa (Quast et al. 2013).

Cyanobacterial Community Composition by Genetic Analysis

The present project provided funding to collect significantly more samples than funds to process all of them for genetic analyses. The information provided is an overview to those analyses completed under the current project phase, though additional analyses may be conducted under future contracts. The data discussed herein pertain to metagenome sequencing of the Clear Lake surface communities (Figures 10 & 11).

Five stations (Stations 1, 4, 5, 7, and 9) from August 28, 2020 were sequenced for the construction of prokaryotic metagenomes. Computational extraction of 16S and 18S sequences from the resulting metagenomic reads using the program PhyloFlash revealed high community similarity across the five stations sampled (Figure 10), although it yielded limited information on microbial eukaryotes (the purpose of the targeted 16S and 18S tag sequencing). Interestingly, Station 9 (Lower Arm) had a notably higher proportion of cyanobacteria compared to the other four stations in both 2020 and 2021 which was consistent with visual assessment during field work.

Five high quality (> 50% completion, < 5% contamination according to CheckM) cyanobacterial metagenome-assembled genomes (MAGs) were assembled from the samples: *Dolichospermum circinale, Lyngbya robusta, Planktothrix sp.,* and two *Microcystis spp.* For the purposes of this report, the latter will be referred to as *Microcystis sp.* A and *Microcystis sp.* B. *L. robusta* was the most common MAG at three out of the five stations, which is consistent with visual field observations and microscopic analysis of samples taken the same day as the metagenome samples (Figure 11A). *D. circinale* and *Planktothrix sp*. were both present at all five stations but in lower amounts than *L. robusta* and the two *Microcystis* MAGs.

Stations 1, 4, 5, 7, and 9 were again sequenced for metagenomes in 2021. Similar to 2020, the program PhyloFlash revealed relative similarities between stations (Figure 10). Cyanobacteria made up a considerable proportion of the microbial community in 2021 as well as 2020, with Station 9 consistently having higher cyanobacterial relative abundances than the others. The cyanobacterial order Synechococcales was present in 2021, however was not detected in 2020 (Figure 10). There were also slight differences in the composition of the heterotrophic bacterial communities between 2020 and 2021. The order Burkholderiales was found in higher proportions in 2021 than in 2020.

Eleven high quality (> 50% completion, < 5% contamination according to CheckM) cyanobacterial MAGs were assembled from the metagenomic reads in 2021, indicating that the cyanobacterial community was more diverse in August of 2021 than in August of 2020. All genera that appeared in 2020 were also present in 2021 (*Dolichospermum, Planktothrix, Lyngbya,* and *Microcystis*). In 2021, *Geminocystis aponina, Nodularia spumigena, Sphaerospermopsis kisseleiania,* as well as two *Pseudanabaena* and three poorly described *CACIAM-69d* MAGs were present. *Microcystis* dominated the cyanobacterial community at Sites 1 and 9. At the three sites where *Microcystis* did not dominate, there was much more diversity within the cyanobacterial community.

Metagenomic analysis of samples from Clear Lake confirmed cyanobacterial dominance over multiple time scales. The appearance of multiple *Microcystis* MAGs in 2020 indicates the possibility of subpopulation dynamics which may play a role in toxin production by *Microcystis.* Preliminary searches for toxin production genes in the 2020 MAGs have indicated that *Microcystis* was the primary microcystin producing cyanobacterial genus in Clear Lake during each of the survey periods.

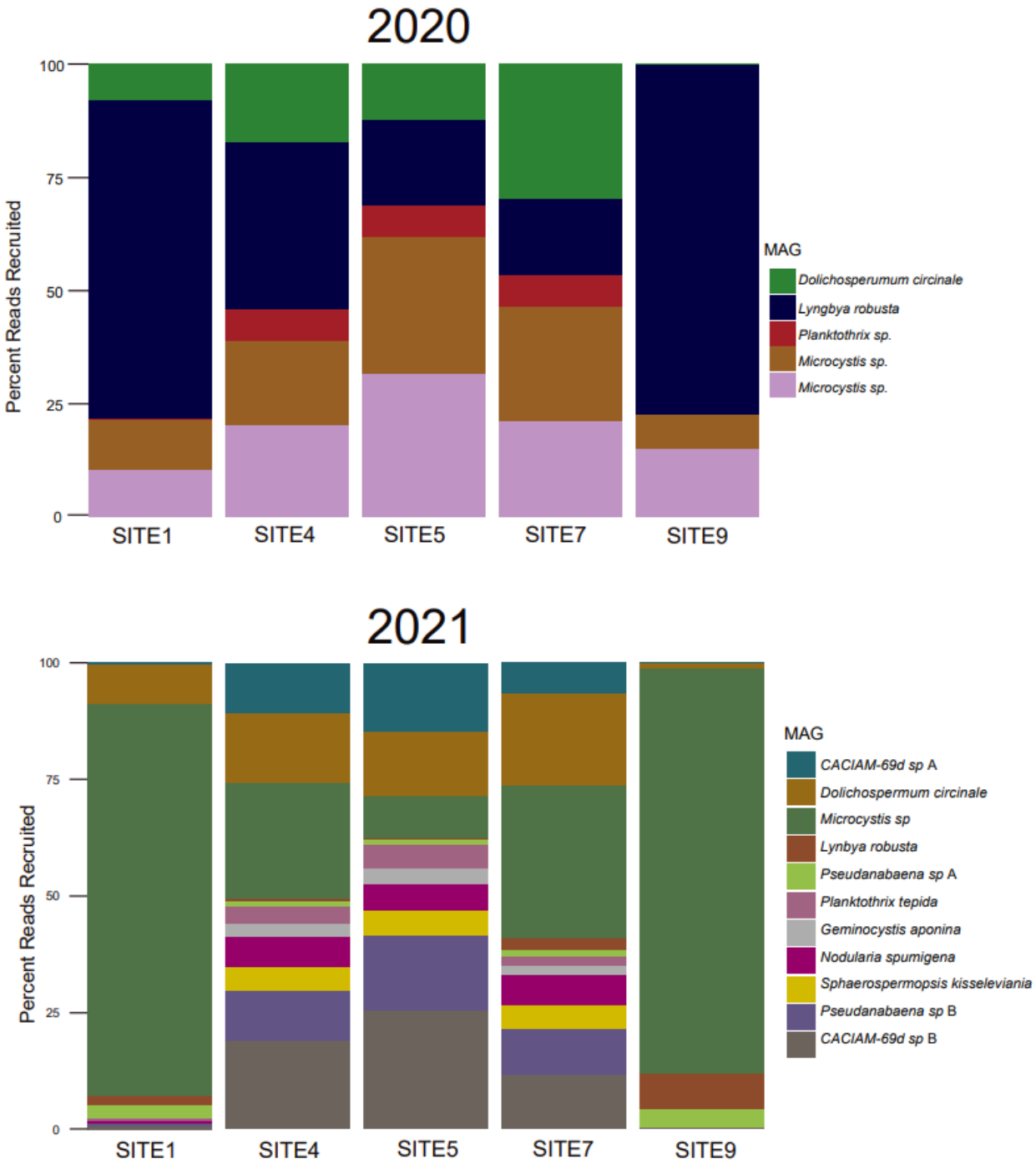

Figure 11. Percent reads recruited of cyanobacteria in 2020 and 2021. Percent recruitment is the number of reads mapped to a bin divided by the total number of reads in a sample, which indicates the composition of the cyanobacterial community.

Physiochemical Variability in Clear Lake Across Multiple Temporal Scales

Nutrient concentrations in Clear Lake varied across both spatial and temporal scales, with the most notable variations occurring over the monthly to seasonal scales. In 2020, sampling occurred during the month of August on an approximately bi-weekly basis. During this sampling effort, total nitrogen concentrations showed small variations over space and time with overall concentrations in August ranging from 0.40 mg N/L to 0.56 mg N/L (Figure 12A). Total phosphorus showed greater changes in concentration during this period with observed concentrations ranging between 0.07 mg P/L and 0.47 mg P/L (Figure 12B). Interestingly, and somewhat surprisingly, total phosphorus concentrations were generally lowest in the Lower Arm and highest in the Upper Arm during any given sampling event. Perhaps unsurprisingly, larger overall variations in nutrient concentrations were observed in 2021 when sampling occurred on a monthly basis for five months. Total nitrogen concentrations ranged between 0.42 mg N/L to 0.82 mg N/L between the months of June to October (Figure 12C), while total phosphorus concentrations ranged between 0.10 mg P/L and 0.59 mg P/L (Figure 12D). Total nitrogen concentrations in the Lower Arm peaked between July and September, followed by a decline in October, while total nitrogen concentrations peaked at most other stations in the Upper and Oaks Arms in October (Figure 12C). The Lower Arm also showed deviations from most of the other stations in the lake in total phosphorus concentrations, with concentrations in the Lower Arm generally being lower than the other stations, and showing a precipitous drop in concentrations between September and October that were not observed at the other stations (Figure 12D).

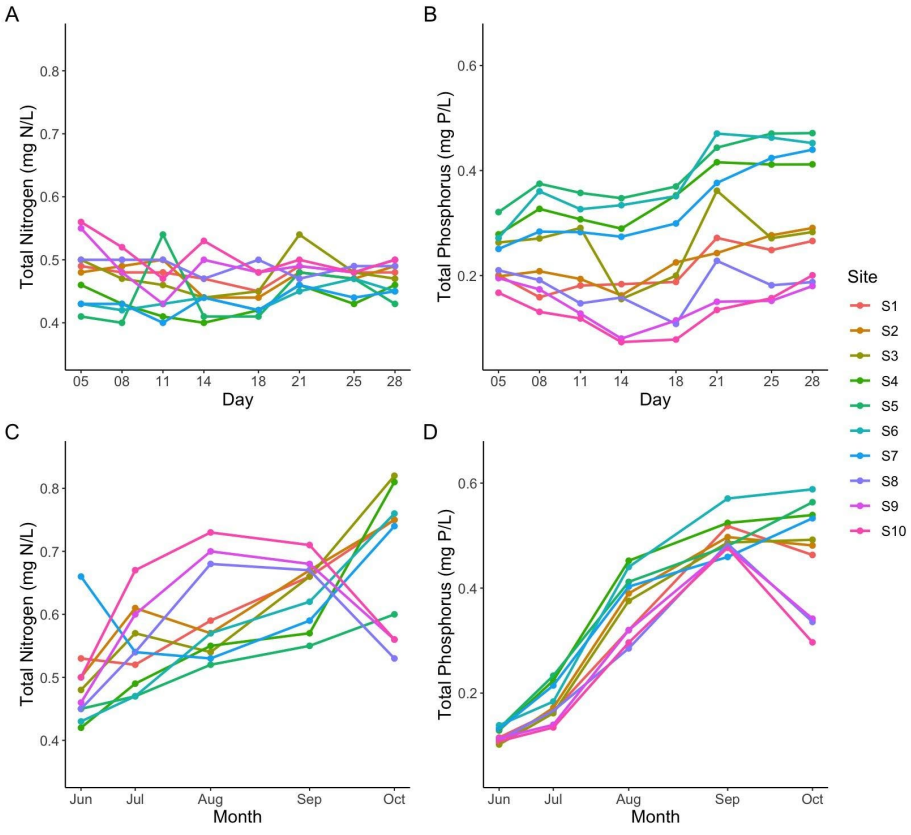

Figure 12. Surface water concentrations of total nitrogen and total phosphorus in 2020, panels A and B, and in 2021, panels C and D.

The ratio between total nitrogen and total phosphorus indicated that Clear Lake is consistently nitrogen limited. Nutrient ratios (calculated by mass) were consistently below the Redfield ratio of 7.22, which is considered balanced for algal growth. This limitation was observed at all stations but one in both 2020 and 2021 (Figure 13). Interestingly, the arms of the lakes generally clustered together with the Lower Arm generally showing the highest N:P ratios (indicating less N-limitation) and the Upper Arm showing the lowest N:P ratios.

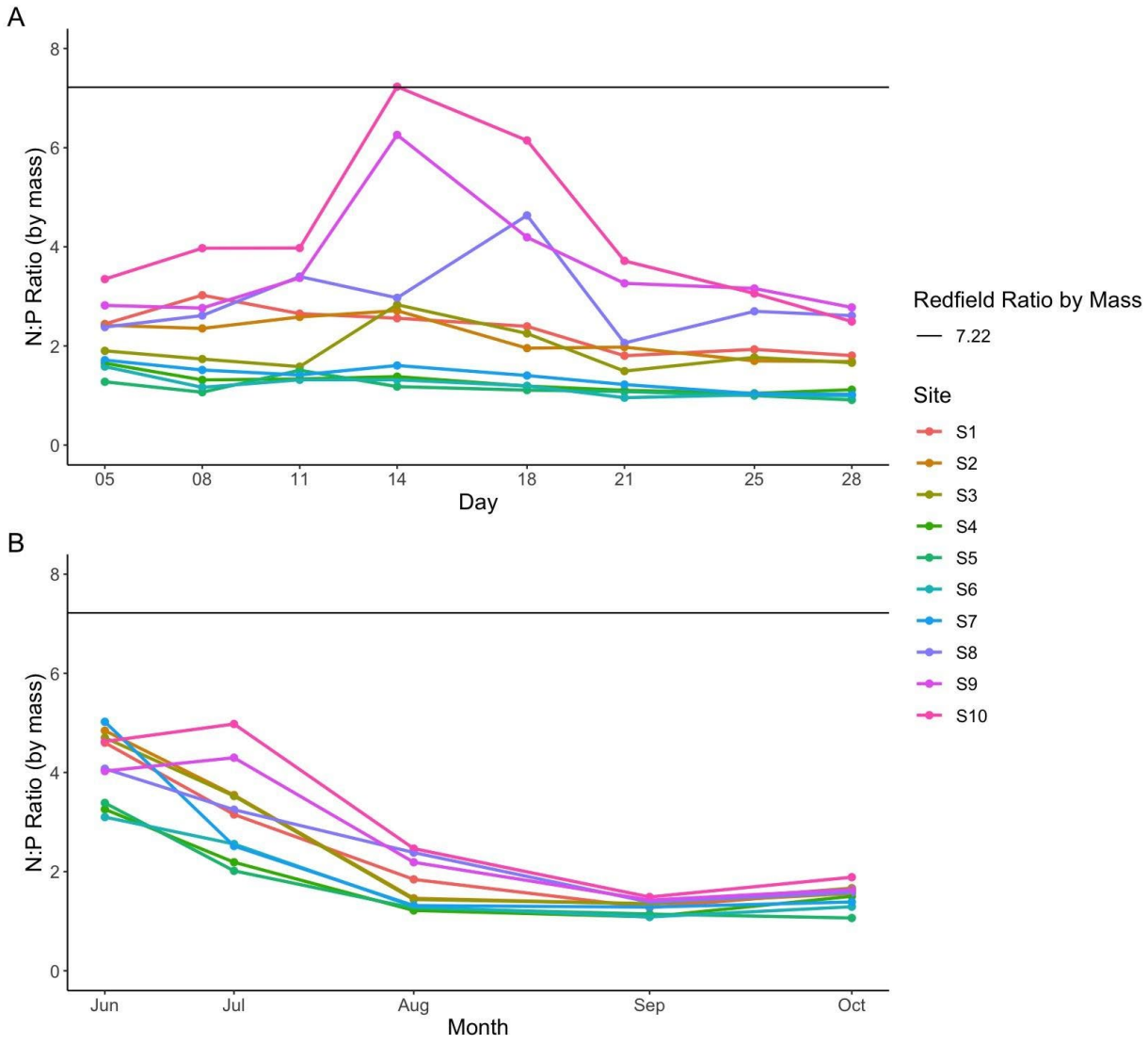

Figure 13. Surface water ratios of total nitrogen to total phosphorus by mass in 2020, panel A, and in 2021, panel B.

Variations in surface water temperature and dissolved oxygen concentrations were observed across and within surveys in August 2020, surface water temperatures ranged between 24.9°C and 29.4°C (Figure 14A). A larger amount of variation was observed in dissolved oxygen concentrations during this same period, with oxygen saturation ranging between 71% and 220% (Figure 14B). These temporal changes indicate a highly dynamic water column processes with respect to oxygen concentration. Highest surface water temperatures were observed across all stations on August 14, 2020, which also corresponded with highest dissolved oxygen concentrations at most stations. Lower temperatures and dissolved oxygen saturation values were observed across the lake between August 18-21, 2020, followed by a stabilization in temperature and slight increase in dissolved oxygen saturation during the observations on August 25 and August 28, 2020 (Figure 14 A, B). These observations correspond with the observed handheld temperature profiles collected at each station (Figure 15), where the water column was well mixed at most stations between August 5-8, 2020, followed by a period of thermal stratification between August 11-18, 20208. Profiles indicated that the water column was well-mixed on August 21, 2020, followed by the re-establishment of stratification at most stations (Figure 15).

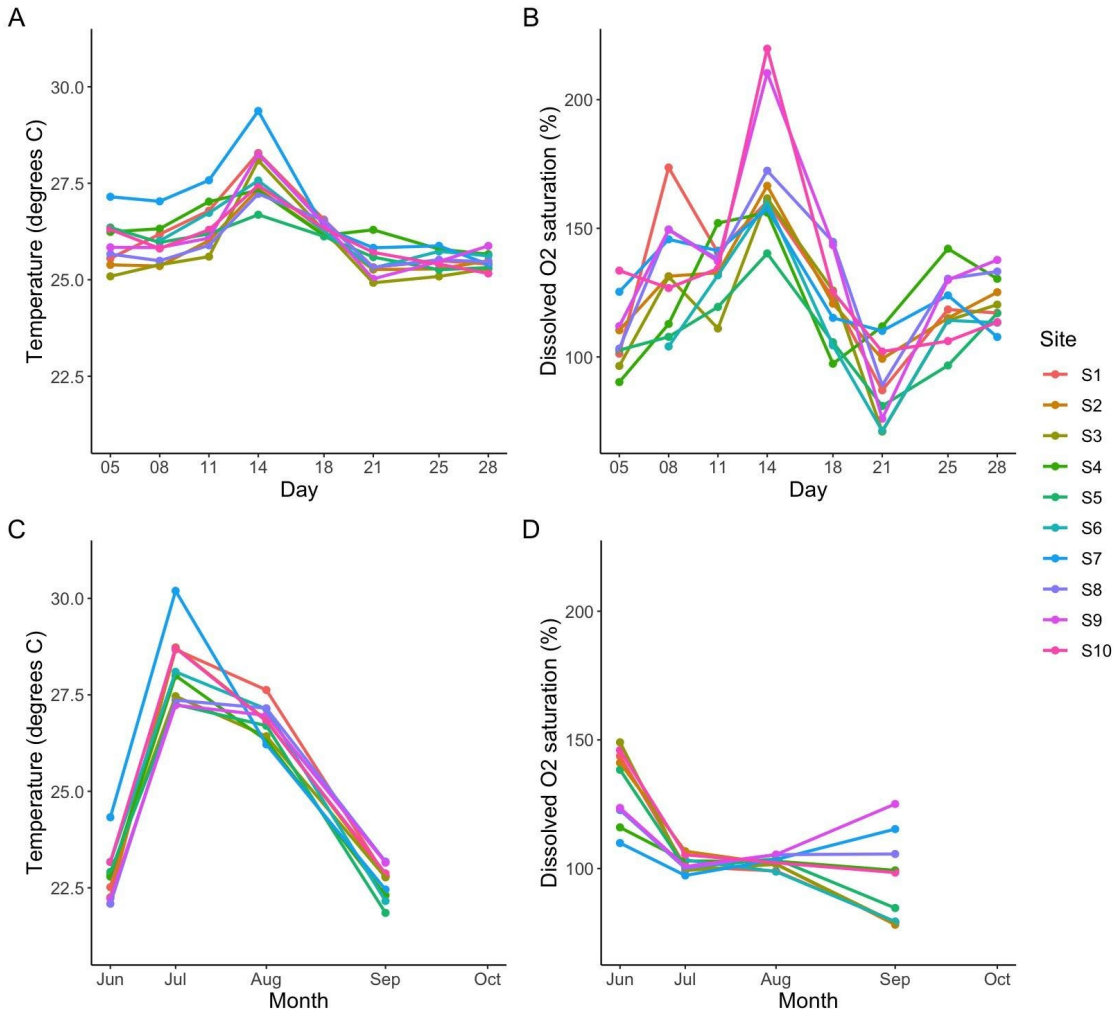

Figure 14. Surface water (0.5 m) temperature and dissolved oxygen concentrations in 2020, panels A and B, and in 2021, panels C and D.

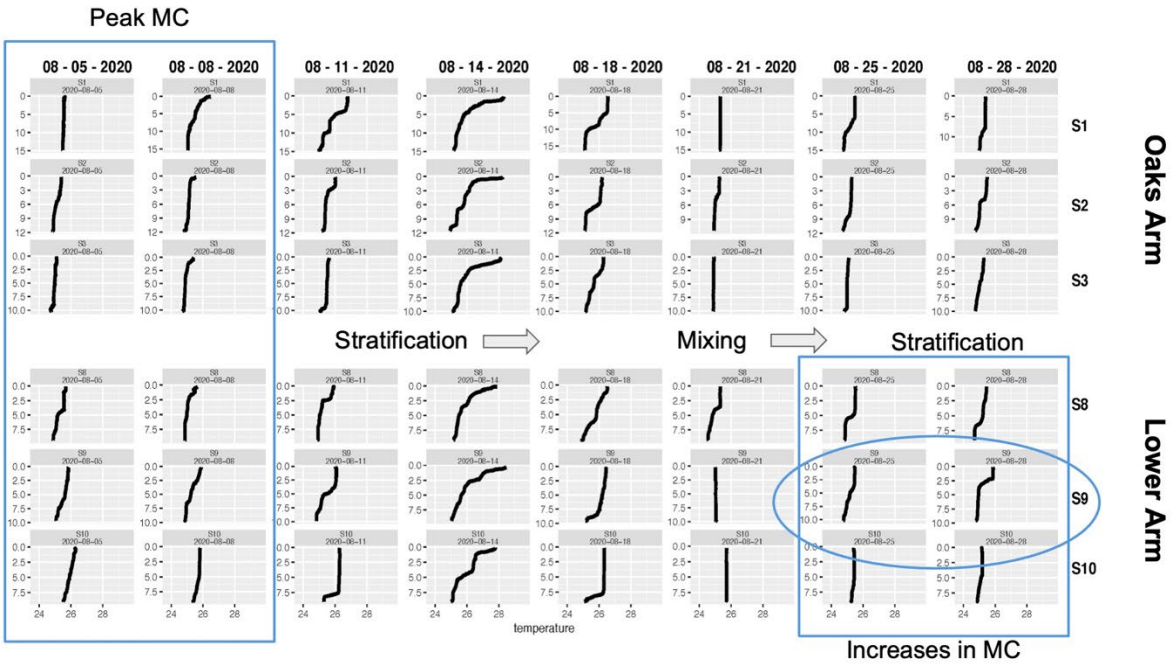

Figure 15. Temperature profiles collected through the month of August 2020 in the Oaks and Lower Arms of Clear Lake showing the development of water column stratification, followed by mixing, and a second period of stratification, particularly in the Lower Arm.

Unsurprisingly, a larger range in surface water temperatures was observed in 2021 between the months of June and September. Instrument failure resulted in lost observations in the month of October. Observed surface water temperatures ranged from 21.9°C and 30.2°C (Figure 14C). Maximal temperatures were observed in July, followed by a slight decline of surface temperatures in August, and a larger decline in September. Dissolved oxygen saturation ranged between 78% and 149% (Figure 14D). Oxygen saturation was maximal at most stations in June, followed by a period of relative stability between July and August. Slight declines in dissolved oxygen saturation were observed at most stations in the Oaks and Upper Arms, while a slight increase was observed at station 9 in the Lower Arm and station 7 (Soda Bay) in the Upper Arm (Figure 14D).

Relationships Between Environmental Conditions, Cyanobacteria Blooms, and Microcystins

Spearman rank correlation was used to examine the associations between total, particulate and dissolved microcystins, and measured biological and physiochemical parameters for the entire data set (2020 + 2021), and for each individual year (2020 and 2021). Among the strongest positive correlations ($p < 0.05$) was the positive correlation between microcystins in all fractions (except dissolved in 2021) and total nitrogen concentrations (Table 3). These correlations were particularly strong in the entire data set (2020 + 2021), and in 2020. Similarly, significant positive correlations were observed with N to P ratios and microcystin concentrations in all fractions in the full dataset and in 2020, though not in 2021. Together, this indicates a general positive relationship between microcystin concentrations and reduced nitrogen limitation throughout the lake. Positive correlations were also observed between all fractions of

microcystins and chlorophyll a across the combined and individual years, though the strength of the correlation varied by year (Table 3). Total phosphorus negatively correlated with dissolved microcystins in the entire data set and in 2020, but this relationship was not observed in 2021 alone. Total phosphorus was also negatively correlated with total and particulate microcystins in 2020, but not in the full dataset or in 2021. Interestingly in 2020, temperature exhibited a negative correlation with all fractions of microcystins, while also exhibiting positive correlations with dissolved oxygen. This relationship was not observed when examining 2021 alone.

Table 3. Spearman rank order correlation results between Total Microcystins, Particulate Microcystins or Dissolved Microcystins, and measured physiochemical parameters. These analyses were conducted using all years combined and by individual year. Bolded values are significant at P ≤ 0.05; n is the number of pairwise comparisons.

2020+2021							
	Chl a	TP	TN	Temp	DO	TN:TP	*n*
Total MC	**0.59**	-0.12	**0.66**	-0.11	-0.07	**0.37**	118-130
Particulate MC	**0.68**	0.05	**0.74**	-0.13	**-0.19**	**0.22**	118-130
Dissolved MC	**0.19**	**-0.4**	**0.21**	**-0.19**	**0.19**	**0.46**	118-130
2020							
	Chl a	TP	TN	Temp	DO	TN:TP	*n*
total	**0.53**	**-0.66**	**0.66**	**-0.29**	**0.16**	**0.7**	79-80
particulate	**0.64**	**-0.57**	**0.66**	**-0.4**	**0.08**	**0.62**	79-80
dissolved	**0.52**	**-0.66**	**0.66**	**-0.27**	**0.16**	**0.7**	79-80
2021							
	Chl a	TP	TN	Temp	DO	TN:TP	*n*
total	**0.39**	0.09	**0.44**	0.11	-0.06	0.04	39-50
particulate	**0.37**	0.11	**0.44**	0.14	-0.08	0.02	39-50
dissolved	**0.4**	-0.11	0.22	-0.1	0.08	0.14	39-50

Instrumented Measures

Whole-lake WireWalker Observations 2020 and 2021

Sensor data collected using the WireWalker in August 2020 and for multiple months in 2021 provided an extremely information-rich dataset for our ongoing analyses. An overview of the data for 2020 is provided in Figure 16 and represents a condensed view of thousands of sensed values across multiple chemical/physical parameters taken throughout the nearly month-long study. Wind speed and direction collected from a meteorological station on the lake are also presented for the period that the instrument was deployed (Figure 16A). Wind direction is shown by the orientation of each vector along a line of time, while wind speed is depicted as the length of each vector. Wind direction was predominantly northwesterly during August 2020 (the typical wind direction on the lake; see circular summary of wind direction and magnitude on the right of Figure 16A) but short periods of wind reversal occurred (especially noticeable as upward-pointing vectors during mid-August and twice near the end of August). Periods of quiescent winds were also observed but are difficult to visualize in the depiction because they are displayed as vectors of zero magnitude in the figure.

Periods of calm winds can be detected in the condensed data visualization of Figure 16 as small white areas in the panel of depth of the instrument versus time (Figure 16E). Closely packed teal lines indicate the vertical position of the instrument as it moves up and down the mooring wire. The WireWalker moves down the wire only when wave action is sufficient to engage the internal rachet mechanism. When wave action is insufficient, the instrument stops at whatever depth it occupies at that time (but continues sensor measurements) until waves are again sufficient to re-activate the rachet (i.e., depth of the instrument remains constant during quiescent periods). This situation ceases the vertical profiling that occurs when the instrument moves, but it provides and extremely useful time stamp of periods when winds are very light or calm. Periods of calm winds would be expected to affect biological processes that would become apparent as patterns in some sensed parameters. For example, dissolved oxygen concentrations may be expected to decrease, especially in deep water, when calm winds decrease water column mixing and microbiological activity depletes oxygen at and near the bottom of the lake.

At the resolution of the data presented in Figure 16, some general trends that occurred across the near-month deployment in August 2020 are apparent. Note that the ranges of temperatures observed throughout the water column (Figure 16B) were much smaller for August 4-9 than for other periods. Given that the instrument moves from near-surface to near-bottom each movement cycle, the results indicate well mixed water column during that period (i.e., the water column was nearly isothermal during that period). Conversely, the periods of August 8-10, 15-18, 22-25, and 27-28 exhibited rather large ranges of temperature across the depth range of the instrument, indicating that water temperature near the surface of the lake was significantly greater than near the bottom. That information implies that the latter periods represented times of the development of water stability (i.e., little to no vertical mixing of the water column).

Also obvious at the level of temporal resolution in Figure 16 is that the ranges observed for dissolved oxygen were greater for the four periods of water column stability than for the intervening time periods (Figure 16D). The most plausible explanation for this pattern is that periods of calm winds (and therefore water column stability) resulted in the rapid utilization of

dissolved oxygen, presumably at depth, while high oxygen concentrations in near-surface waters were maintained by photosynthesis-related oxygen production.

What is the importance of these WireWalker observations for understanding algal and cyanobacterial blooms in Clear Lake? The alternating periods of calm and well mixed waters implied by the data, and concomitant changes in water chemistry, appear to be creating alternating periods low dissolved oxygen and high dissolved oxygen in the water column. These changes should be particularly acute at and near the sediments. Therefore, the instrument recorded large ranges of dissolved oxygen concentrations observed during periods of high water column stability, as shown in Figure 16B, D. The significance of these findings are that if anoxic conditions develop at the sediment surface during periods of stable water column structure, those conditions may enhance phosphorus release from the sediments (a chemical process enhanced under anoxic conditions). Subsequent water column mixing may then return those nutrients released during anoxia into the near-bottom water up into the lighted water of the lake where they can fuel or maintain algal/cyanobacterial blooms. The rapidity and frequency of these alternating patterns, enhanced by high rates of decomposition in the sediments, could be a major mechanism for recurring blooms in Clear Lake throughout the summer. While this process has been proposed for Clear Lake which is known to be a polymictic lake, our data provide convincing data for this phenomenon, and the frequency of this process (see below).

The pattern of chlorophyll fluorescence during August 2020 (Figure 16C) was temporally noisy. Interestingly, very high values of chlorophyll fluorescence were often observed during "quiescent" periods. Since the appearance of these high values are greater than increases that could be explained by cell growth, they presumably indicate the accumulation of algae and/or cyanobacteria at particular depths during quiescent periods in the lake. Sharp "spikes" in chlorophyll concentrations sometimes observed near the bottom of the lake presumably are a consequence of sinking of phytoplankton, possibly during bloom senescence.

The rich dataset collected by the WireWalker and its instruments also provided valuable insight with respect to lake dynamics on much finer time scales (Figure 17, 18, 19, 20) than the nearly month-long deployment shown in Figure 16. Expansion of the time scale of Figure 16 to examine an approximately 24-hour time period provided insight into the rapidity of variances in the dynamics of Clear Lake's water column (Figure 17). The time slice revealed rapid and repeated vertical transits of the WireWalker for the first few hours as shown by the tightly spaced teal lines depicting instrument depth. Note that most sensed parameters during this time period remained relatively stable, indicating a well-mixed water column (i.e., little change in the parameters vertically in the water column). Following this period of rapid movement of the WireWalker, the instrument made only a single vertical transit between the period ≈20:35 and 22:15). During that transit, the instrument stalled at 1-2 m depth, and then again at 2.5 m depth. The instrument then resumed vertical movement at approximately 21:45. Note that as the WireWalker moved into deep water at ≈21:45, it recorded low dissolved oxygen in the deep water that was not observed when the instrument was moving quickly down and up the wire (dark blue line depicting dissolved oxygen in Figure 17).

Two important pieces of information can be garnered from this pattern. First, periods of water column mixing/stability may be quite short and change rapidly in Clear Lake. Second, the response of water chemistry (most notably dissolved oxygen) can be very rapid (within hours during the August 2020 deployment), indicating that oxygen utilization at the sediment surface

(and presumed phosphorus mobilization due to anoxia) may take place very rapidly once water column mixing slows.

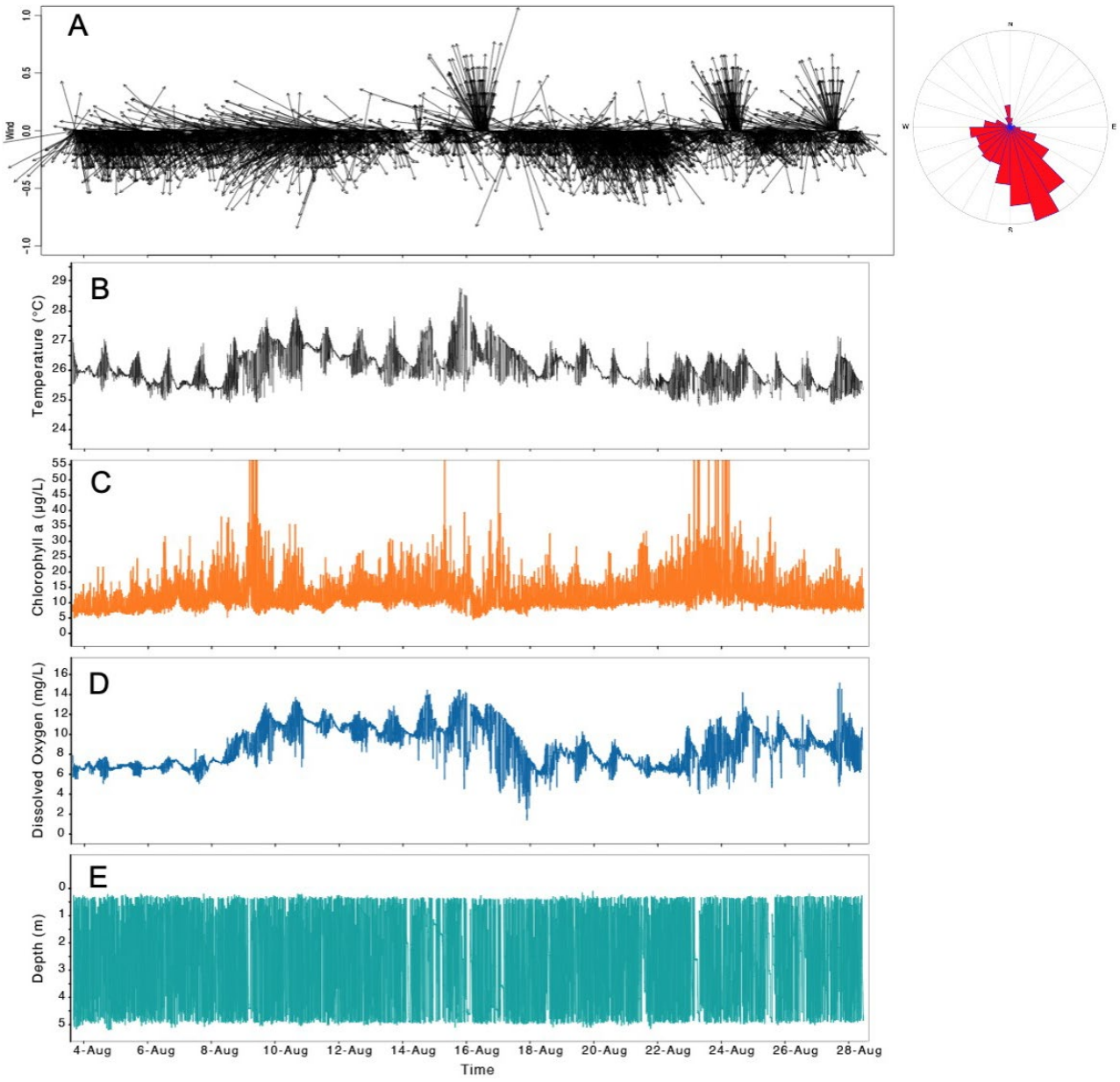

Figure 16. In situ data from the WireWalker moored at Station 4 in 2020 for the entire deployment period of August 3-28, 2020. Wind direction and magnitude is shown in panel A, temperature in panel B, Chlorophyll in panel C, Dissolved Oxygen in panel D, and Depth in panel E.

Further examination of the August 2020 WireWalker dataset provided observations that are consistent with the scenario described above (i.e., intermittent periods of water column stability and mixing, and consequent changes in water column chemistry, particularly dissolved oxygen). Figure 18 shows a depiction of dissolved oxygen in the water column of Clear Lake from the period August 3-19, 2020. Concentrations (down-wire data only) are shown in this Figure as discrete squares at the depth of each measurement. The very high density of the measurements

provides “depth contours” of the data. Note that dissolved oxygen concentrations for approximately the first 5 days of this time segment (August 3-9) revealed relatively low dissolved oxygen concentrations distributed relatively uniformly throughout the water column, followed by a period (August 9-15) of higher concentrations also distributed relatively uniformly throughout the water column. However, the thin “white gaps” during the time period outlined by the green box (August 15-18) were periods when the WireWalker stopped moving vertically (i.e., periods of low wave action, calm winds).

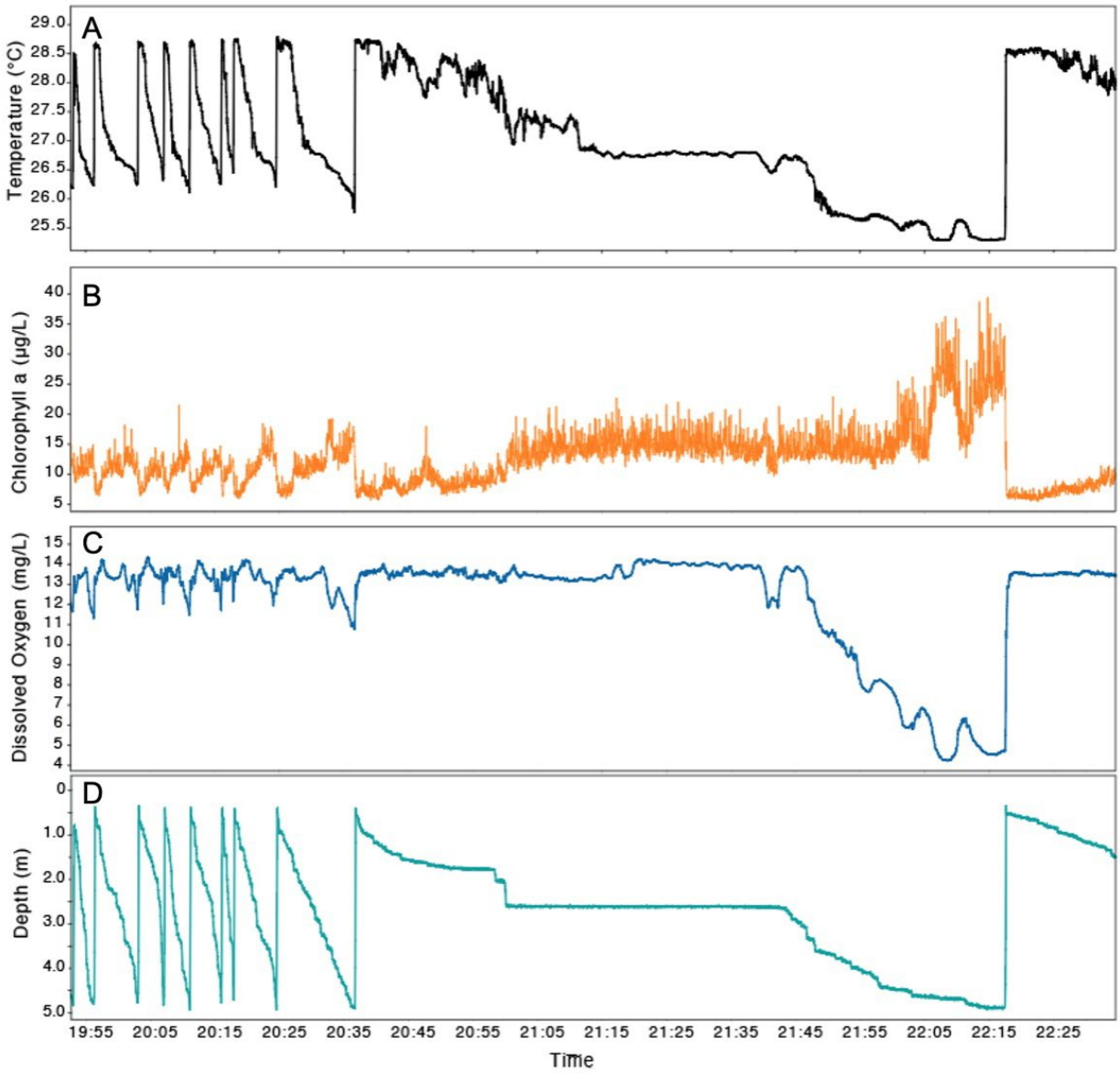

Figure 17. Zoomed in in situ data from the WireWalker moored at Station 4 in 2020 for 8/15/2020 in the afternoon and evening. Temperature is shown in panel A, Chlorophyll in panel B, Dissolved Oxygen in panel C, and Depth in panel D.

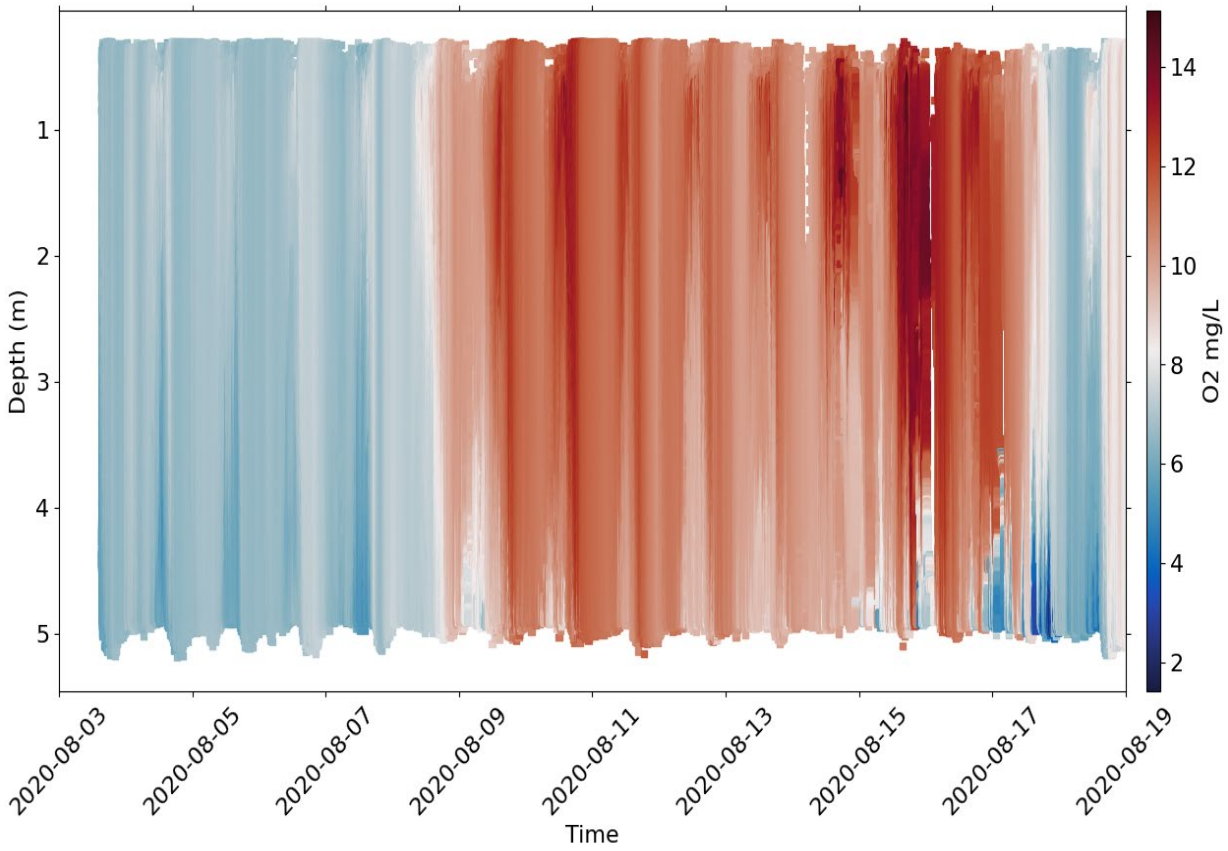

Figure 18. Dissolved oxygen concentrations with depth, presented as contoured data, from August 3 to August 19, 2020, at a station near the confluence of the three Arms of Clear Lake determined using the WireWalker. The region outlined in the green box is expanded in Figure 19 below. Note the slight "gaps" (small white vertical areas) in parameters, indicating that the WireWalker was stationary in the water at those times (i.e., wave action was insufficient to engage the rachet mechanism of the device which forces the instrument down the deployment wire).

Expansion of the latter time segment (August 15-18) documented when the instrument remained stationary in the water column (indicated by swaths of horizontal measurements in Figure 19). The white gaps occur because the instrument is not traversing up and down the wire rapidly, rather the measurement are concentrated at the particular depth where the instrument stalled. Several of the periods when the instrument was not moving were followed by significantly lower dissolved oxygen concentrations in deep water than observed prior to the calm conditions (indicated by green ovals in Figure 19). This pattern of calm periods followed by low dissolved oxygen in deep water is consistent with the idea that periods of low wave activity rapidly resulted in low dissolved oxygen concentrations near or at the sediment surface. Wave action following those quiescent periods quickly dispersed oxygen once more throughout the water column. Assuming phosphorus is released from the sediments during those intermittent hypoxic/anoxic events, its distribution into lighted surface waters may provide frequent nutrient replenishment to phytoplankton in surface waters. While this scenario is consistent with conjecture regarding blooms in Clear Lake, the WireWalker provided clear evidence of that behavior, and information on how remarkably rapid these events may take place.

Whole-lake EcoMapper observations 2020 and 2021

A difficult task faced by researchers and monitors studying Clear Lake is the sheer size of the lake. Limited resources and personnel make it impossible to obtain a whole-system understanding of chemistry, physics and biology that characterize the lake. Near synoptic measurements using the sensors carried by the EcoMapper provided both excellent contextual background for the whole lake within a relatively narrow sampling window (transects along the main axes of all arms of the lake in 3 days, one per day), thereby aiding interpretation of the limited number discrete analyses that we were able collect and process in our research programs (see information on Discrete Sample Collection). As noted above, only Upper Arm could be conducted in October 2021 because floating debris caused by a severe storm in the region presented an entanglement hazard for the vehicle.

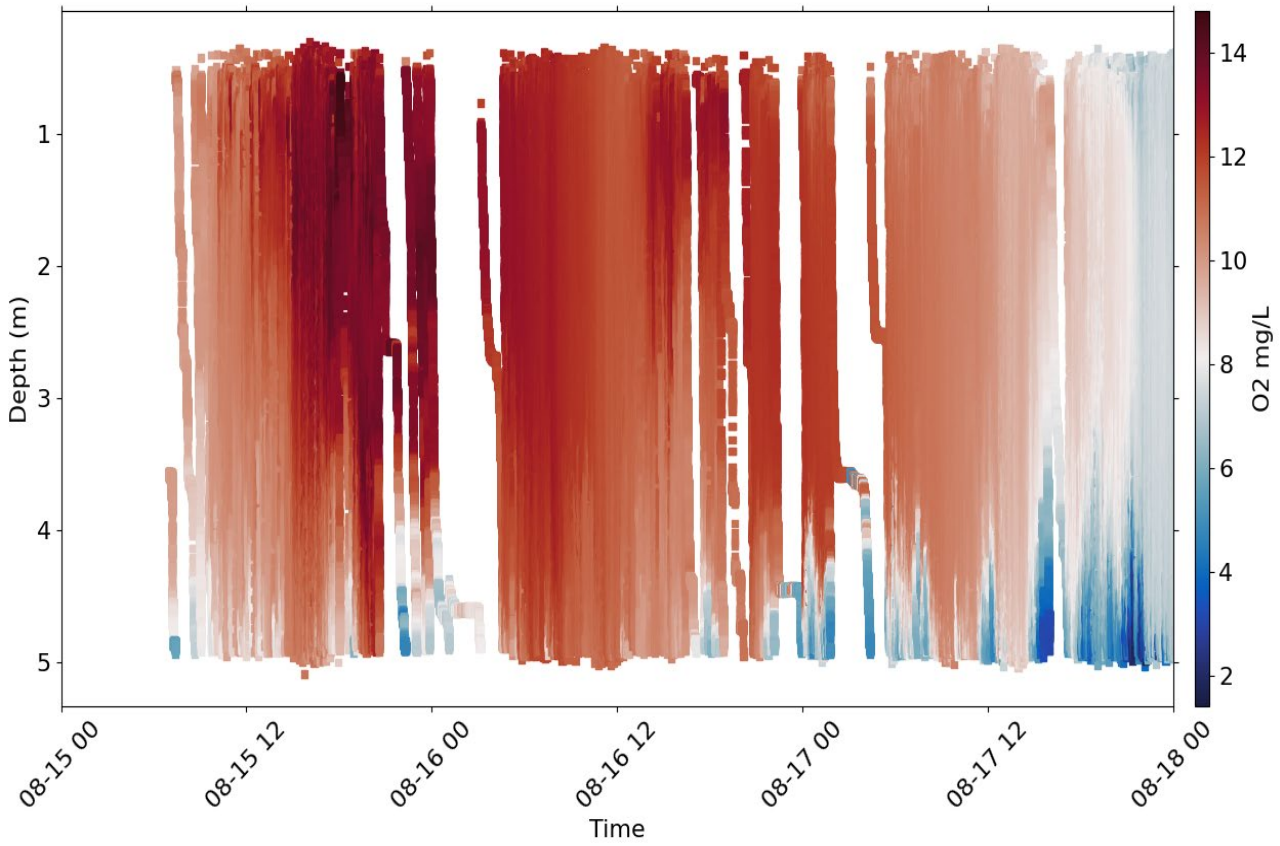

Figure 19. Expanded view of dissolved oxygen concentrations with depth from August 15 to August 18, 2020, at a station near the confluence of the three Arms of Clear Lake (time period outlined by green box in Figure 18). Expansion of the x-axis (time) reveals changes in dissolved oxygen with depth at times when the WireWalker was not moving down the deployment wire (periods of horizontal orientation of sensed data in the Figure indicating that the WireWalker remained at a particular depth during those time periods. Note that those periods are often associated with hypoxia in deep water when the instrument begins moving again (compare dissolved oxygen concentrations in deep water of the lake on August 15 (high wave action) relative to dissolved oxygen concentrations in deep water at the times indicated by the green ovals). Calms waters (i.e., low wave action, presumably times of low vertical mixing of the lake) allowed the rapid depletion of oxygen at or near the bottom of Clear Lake, which was then dispersed throughout the water column when wave action returned.

Data obtained from the 2020 deployment indicates the extreme differences in the chemistry and biology of Clear Lake, across the expanse of all three arms of the lake, demonstrating the usefulness of the robotic instrumentation in capturing differences at the whole-lake scale (Figure 20).

Temperature along the main axes of the three arms of the lake (Figure 20, top row of panels) revealed Upper Arm to be somewhat uniformly warmer than the other arms of the lake during the study, with generally lower near-surface temperature towards the east end of Upper Arm and highest water temperature towards the western (and more shallow) end. Lower Arm displayed the coolest water temperatures overall, while water temperature in Oaks Arm was intermediate between Upper and Lower Arms. Note that the approximately top 1 m of the water is not depicted because the robotic vehicle is programmed to not enter that layer in order to avoid boat strikes.

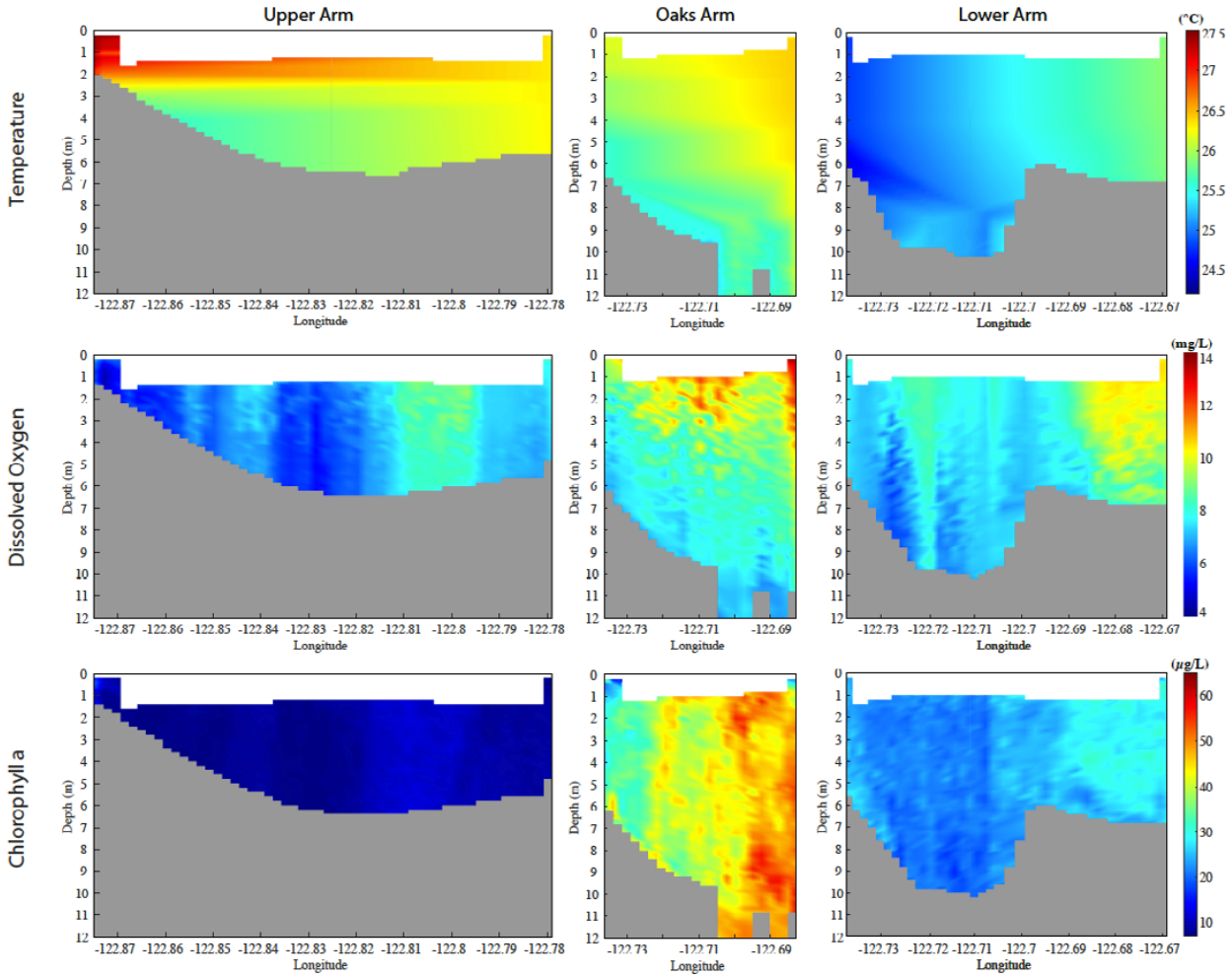

Figure 20. Whole lake EcoMapper transects conducted in 2020 (Upper Arm: August 5; Lower Arm: August 6; Oaks Arm: August 7) showing temperature, dissolved oxygen and chlorophyll a.

Chlorophyll fluorescence ranges (a proxy for total phytoplankton biomass; Figure 20 lower row of panels) were very different in the three arms of the lake during the August visitation in 2020. Upper Arm exhibited "low" values of chlorophyll fluorescence that were fairly consistent throughout the arm, relative to values observed in the Oaks and Lower Arms. Note, however, that the lower end of the scale is still approximately 10 µg/L. In contrast to Upper Arm, Oaks Arm exhibited chlorophyll fluorescence values that exceeded 50 µg/L, particularly concentrated towards the eastern end of the arm. Chlorophyll fluorescence values are not directly comparable to extracted chlorophyll concentrations, but these values indicate hypereutrophic conditions, and values in excess of 5X the values observed in Upper Arm during the same period. Lower Arm at the time of sampling exhibited chlorophyll fluorescence values intermediate between Upper and Oaks Arms, and also showed higher values concentrated towards the eastern end of Lower Arm. Patterns of dissolved oxygen concentrations (Figure 20, middle row of panels) in the three arms of the lake somewhat reflected patterns of chlorophyll fluorescence (not surprisingly).

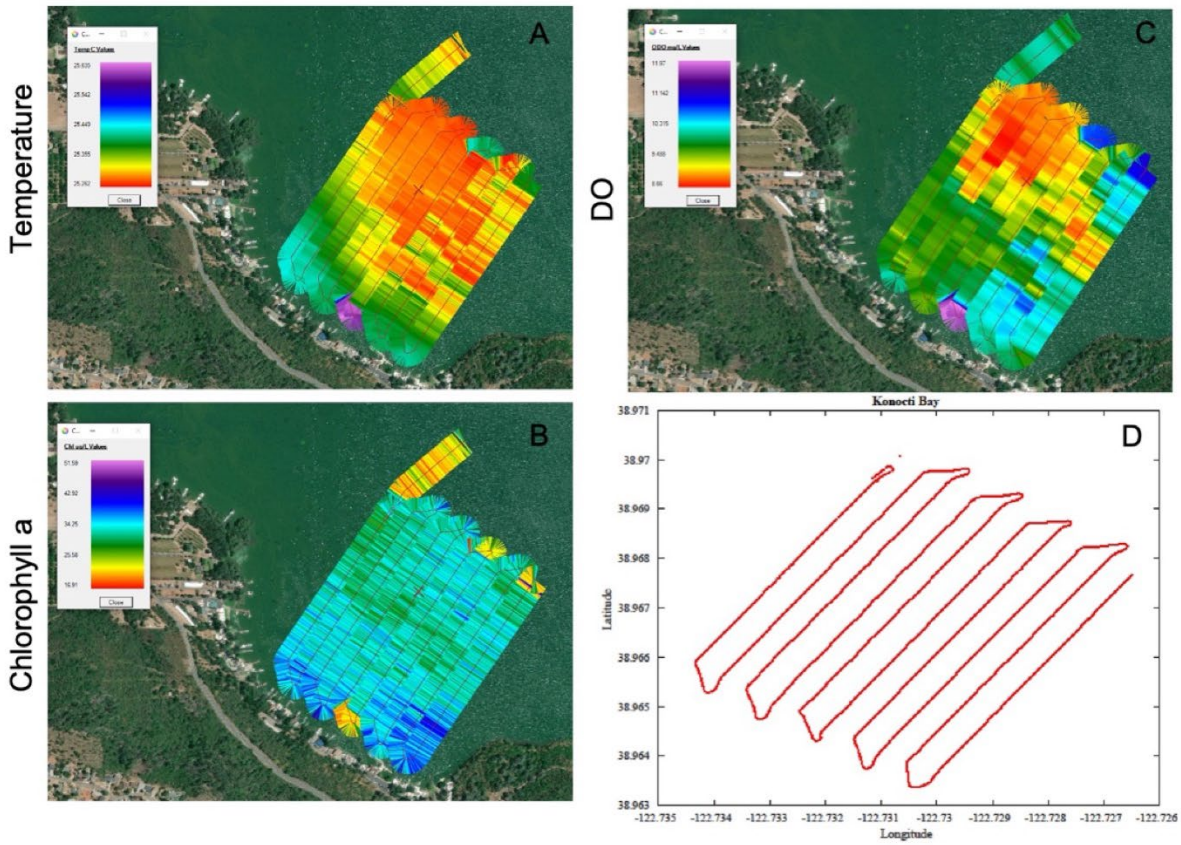

Figure 21. Konocti Bay EcoMapper transects conducted on August 7, 2020 showing A) temperature, B) chlorophyll a, C) dissolved oxygen, and D) the planned EcoMapper transects.

Note that these general patterns of phytoplankton biomass (chlorophyll fluorescence) in the three arms of the lake are not really in keeping with conventional wisdom that cyanobacteria reach highest abundances and dominance in warmer waters. While this generality may hold when examined and averaged across many aquatic ecosystems, Clear Lake (as a whole) did not fit with that general pattern during this study period, presumably indicating the importance of other factors determining phytoplankton biomass across the expanse of Clear Lake.

Paired Drone, EcoMapper, and Discrete Sampling in Konocti Bay, 2020.

The EcoMapper data collected along the main axes of the three arms of Clear Lake provided a synoptic assessment of the large-scale spatial distribution of cyanobacteria and pertinent chemical/physical parameters, but it is less useful for planning the collection of discrete water samples. The latter is thwarted by small-scale spatial heterogeneity (patchiness) in the distribution of cyanobacteria horizontally and vertically that complicates the choice of exactly where to collect a sample. The use of robotics sensing (chemical/physical parameters sensed using the EcoMapper, and imagery collected by the drone) paired with discrete sampling conducted by personnel in boats was conducted in the inner reaches of Konocti Bay in 2020 to investigate this issue.

The EcoMapper was flown at a constant depth of 1.5 m for this mission, in a lawnmower pattern throughout the study area in order to characterize spatial heterogeneity at that depth (Figure 21D). The drone flew overhead during the EcoMapper deployment, capturing imagery of the surface of the water, while simultaneously personnel were deployed to collect discrete water samples at ten stations throughout the study area. Discrete water samples were collected by hand from the surface of the lake where visible patches of cyanobacteria had collected (Figure 22C), and from water adjacent to each aggregate sample but without visible accumulations of cyanobacteria. Water samples were also collected at 1.5 m depth using a Niskin sampler.

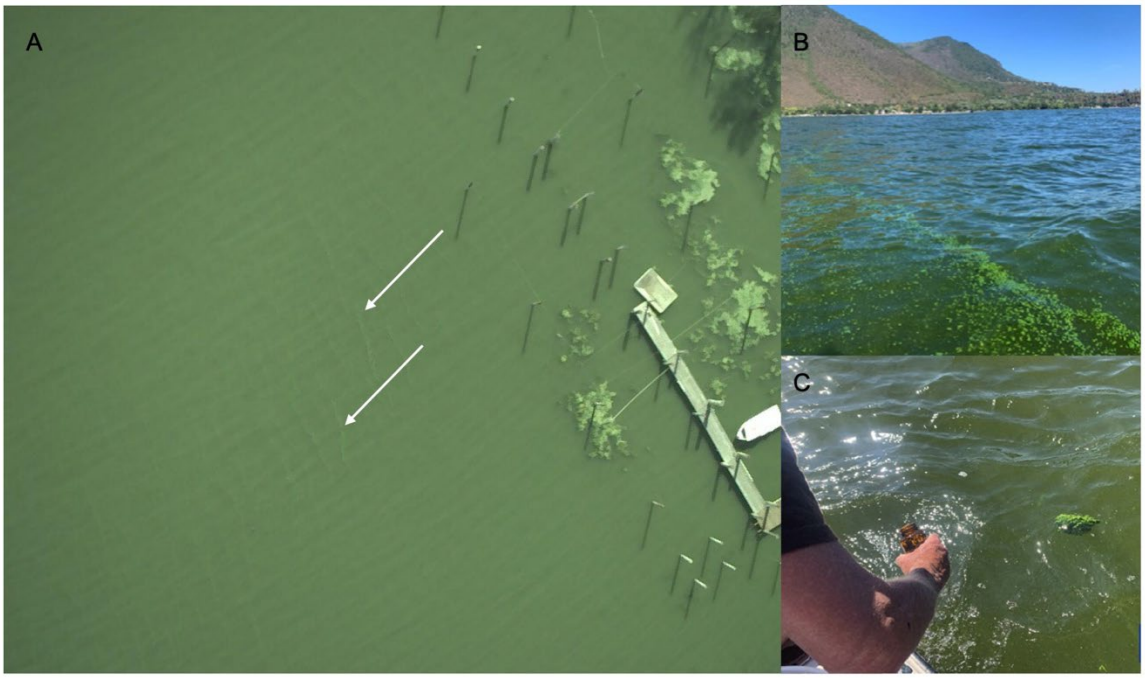

Figure 22. Konocti Bay grid sampling conducted on August 7, 2020 showing A) drone imagery of transect region with surface accumulations of cyanobacteria highlighted with white arrows, B) and C) images of the cyanobacterial biomass accumulations as observed from concurrent ship based discrete sampling.

Contoured patterns of temperature, chlorophyll fluorescence, and dissolved oxygen revealed higher values for all three parameters towards the northwestern region of the study area, but overall only the range of dissolved oxygen was substantial (Figure 21A-C). Drone imagery indicated a different spatial heterogeneity of cyanobacteria at the lake surface (Figure 22A), with long thin streaks of *Microcystis* clumps that formed windrows along the surface of the lake. Sampling of these clumps by hand, sampling at the surface away from these clumps (Figure 22B,C), and sampling at 1.5 m depth using the Niskin sampler yielded very different results across ten stations within the study area (Table 4). Concentrations of microcystins were really two orders of magnitude higher for the *Microcystis* clumps than for the surface water samples collected without visible clumps and from the subsurface samples. Similarly, extracted chlorophyll *a* concentrations in the clumps averaged approximately 170X the values obtained for the surface water samples collected without visible clumps and from the subsurface samples.

Table 4. Microcystin and chlorophyll a results from discrete sampling in Konocti Bay in 2020.

Microcystins µg/L				**Chlorophyll a µg/L**			
Sample	Patch (aggregate)	Non-Patch	Below (1.5m)	Sample	Patch (aggregate)	Non-Patch	Below (1.5m)
1	154.2	2.45	1.42	1	7767	63	76
2	139.6	6.05	1.40	2	6379	132	81
3	124.7	1.88	1.94	3	9047	78	74
4	226.4	2.52	1.94	4	40179	119	76
5	226	2.64	1.91	5	18080	55	97
6	233.8	2.65	1.58	6	16330	78	91
7	84	1.88	1.96	7	10608	98	91
8	163.6	1.98	2.30	8	10575	100	87
9	97	1.36	2.09	9	14210	100	100
10	82.4	2.02	1.81	10	18524	100	97
AVG	153.1	2.54	1.83	**AVG**	15169.9	92.3	87
SD	58.9	1.30	0.29	**SD**	9769.2	23.94	9.71
SE	18.6	0.41	0.09	**SE**	3089.3	7.57	3.07

RECOMMENDATIONS

1. **Continued work is needed to expand the understanding of cyanobacterial diversity in Clear Lake and develop a clear understanding of which taxa have toxigenic potential and under what conditions.**

   Continued molecular analysis can reveal additional details about the diversity of the cyanobacterial and eukaryotic algae diversity in Clear Lake. Importantly, deeper molecular characterization can specifically identify which cyanobacterial taxa in the community have the genetic potential to produce cyanotoxins as well as identifying when these taxa turn on (and off) their toxin production genes. When paired with observations of environmental conditions, this information can be linked to the specific conditions that trigger cyanotoxin production. Additionally, this work can also identify the biological relationships among the microbial species in the lake (mutualism, competitive, etc.) and how these relationships might relate to cyanobacterial bloom formation and toxin production. Collectively, this information will allow for targeted management decisions to be made to mitigate these events.

2. **Cyanobacterial bloom sampling in Clear Lake needs to be carefully designed to address management questions.**

   The spatial heterogeneity of cyanobacterial blooms adds considerable complexity for assessing and monitoring blooms in the lake (e.g., results of small scale sampling in Konocti Bay). It is imperative that specific programmatic goals guide the sampling approach used to characterize toxicity in the lake. Approaches to characterize the average bloom condition in the lake, or to characterize a worst-case exposure scenario will vary and will require different sampling approaches. Determining these goals is fundamental to designing the correct monitoring program and sampling protocols.

3. **Given our improved understanding of the impact of water column mixing on anoxia and potential nutrient release from the sediments, management of cyanobacterial blooms in Clear Lake should consider the importance of internal nutrient loads as well as the influence of external loads.**

   The instrumented measurements in this study have highlighted intermittent wind-quiescent periods as an important factor that may be contributing to the development and/or longevity of large cyanobacterial blooms. Periods of water column mixing/stability may be quite short and switch rapidly in Clear Lake. The resulting changes in water chemistry (most notably dissolved oxygen) can also be very rapid, indicating that oxygen utilization at the sediment surface (and presumed phosphorus mobilization due to anoxia) may take place very rapidly once water column mixing ceases. These pulses appear to provide an additional source of nutrients to the upper water column, likely influencing bloom dynamics. Additionally, discrete sampling efforts that suggested nitrogen limitation is common throughout the lake. These conditions, paired with intermittent internal phosphorus fluxes likely impart a strong driver of cyanobacterial community composition and overall toxin concentrations within the lake. Future management actions in the lake need to consider the combined influence of internal and external nutrient loading as well as dual nutrient control of blooms.

REFERENCES

Alneberg J., B.S. Bjarnason, I. de Bruijn, M. Schirmer, J. Quick, U.Z. Ijaz, et al. 2013. CONCOCT: Clustering cONigs on COverage and ComposiTion. 1–28

Andrews S. 2010. Babraham Bioinformatics - FastQC A Quality Control tool for High Throughput Sequence Data.

Bolger A.M., M. Lohse, B. Usadel. 2014. Trimmomatic: A flexible trimmer for Illumina sequence data. *Bioinformatics* **30**: 2114–2120

Eren A.M., Esen OC, Quince C, Vineis JH, Morrison HG, Sogin ML, et al. 2015. Anvi'o: An advanced analysis and visualization platformfor 'omics data. *PeerJ* **2015**: 1–29.

Eren A.M., E. Kiefl, A. Shaiber, I. Veseli, S.E. Miller, M.S. Schechter, et al. 2021. Community led, integrated, reproducible multi-omics with anvi'o. *Nat Microbiol* **6**: 3–6.

Gruber-Vodicka H.R., B.K.B. Seah, E. Pruesse. 2020. phyloFlash: Rapid Small-Subunit rRNA Profiling and Targeted Assembly from Metagenomes. *mSystems* **5**.

Lane, J.Q., C.M. Roddam, G.W. Langlois, and R.M. Kudela. 2010. Application of Solid Phase Adsorption Toxin Tracking (SPATT) for field detection of the hydrophilic phycotoxins domoic acid and saxitoxin in coastal California. *Limnology and Oceanography, Methods* 8:645-660

Leinonen, R., H. Sugawara, and M. Shumway. 2011. The sequence read archive. *Nucleic Acids Research*, 39(SUPPL. 1), 2010–2012. https://doi.org/10.1093/nar/gkq1019

Li, Y., J. Chen, Q. Zhao, C. Pu, Z. Qiu, R. Zhang, and W. Shu. 2011. Chronic exposure to microcystin may be associated with liver damage in children in the Three Gorges Reservoir Region. *Environ. Health Perspect*. 119:1483-1488

Li D., C.M. Liu, R. Luo, K. Sadakane, T.W. Lam. 2015. MEGAHIT: An ultra-fast single-node solution for large and complex metagenomics assembly via succinct de Bruijn graph. *Bioinformatics* **31**: 1674–1676

Mioni, C.E. and R. Kudela. 2011. Harmful cyanobacteria blooms and their toxins in Clear Lake and the Sacramento-San Joaquin Delta (California). Delta (California) 10:058-150

Nurk S., D. Meleshko, A. Korobeynikov, P.A. Pevzner. 2017. MetaSPAdes: A new versatile metagenomic assembler. *Genome Res* **27**: 824–834. .

Otten, T.G. and H.W. Paerl. 2015. Health effects of toxic cyanobacteria in U.S. drinking and recreational waters: our current understanding and proposed direction. *Current Environmental Health Reports* 2:75-84

Paerl, H.W. and V.J. Paul. 2012. Climate change: Links to global expansion of harmful cyanobacteria. Water Res 46:1349-1363

Peng Y., H.C.M Leung, S.M. Yiu, F.Y.L. Chin. 2012. IDBA-UD: A de novo assembler for single-cell and metagenomic sequencing data with highly uneven depth. *Bioinformatics* **28**: 1420–1428.

Pinkel, R., M.A. Goldin, J.A. Smith, O.M. Sun, A.A. Aja, M.N. Bui, and T. Hughen. 2011. The Wirewalker: a vertically profiling instrument carrier powered by ocean waves. *J. Atmos. Oceanic Technol.,* 28:426-435

Rainville, L. and R. Pinkel. 2001. Wirewalker: An autonomous wave-powered vertical profiler. *J. Atmos. Oceanic Technol.,* **18,** 1048-1051.

Richerson, P.J., T.H. Suchanek, and S.J. Why. 1994. The causes and control of algal blooms in, Clear Lake. Clean Lake Diagnostic/Feasibility Study for Clear Lake, California, Davis, CA

Stewart, I., A.A. Seawright, and G.R. Shaw. 2008. Cyanobacterial poisoning in livestock, wild mammals and birds—an overview. *Adv. Exp. Med. Biol.* 619:613-637

Trevino-Garrison, I., J. DeMent, F.S. Ahmed, P. Haines-Lieber, T. Langer, H. Menager, J. Neff, D. van der Merwe, and E. Carney. 2015. Human illness and animal deaths associated with freshwater harmful algal blooms – Kansas. *Toxins* 7:353-366

Quast, C., E. Pruesse, P. Yilmaz, J. Gerken, T. Schweer, P. Yarza, J. Peplies, and F.O. Glöckner. 2012. The SILVA ribosomal RNA gene database project: improved data processing and web-based tools. *Nucleic acids research*, *41*(D1), pp.D590-D596.

Yeh, Y.C., J. McNichol, D.M. Needham, E.B. Fichot, L. Berdjeb, and J.A. Fuhrman JA. 2021. Comprehensive single-PCR 16S and 18S rRNA community analysis validated with mock communities, and estimation of sequencing bias against 18S. *Environmental Microbiology*. 23: 3240-3250